Elisabeth Rossegger, BSc

Crosslinked Poly(2-oxazoline)-Based Micelles as Drug Depots

MASTERARBEIT

Zur Erlangung des akademischen Grades

Diplom-Ingenieurin

Masterprogramm Technische Chemie

Eingereicht an der

Technischen Universität Graz

Betreuer

Priv. -Doz. Dipl. - Chem. Univ. Dr. rer. nat. Frank Wiesbrock

Institute for Chemistry and Technology of Materials

Polymer Competence Center Leoben GmbH

Graz, Juni 2017

EIDESSTATTLICHE ERKLÄRUNG

Ich erkläre an Eides statt, dass ich die vorliegende Arbeit selbstständig verfasst, andere als die angegebenen Quellen/Hilfsmittel nicht benutzt, und die den benutzten Quellen wörtlich und inhaltlich entnommenen Stellen als solche kenntlich gemacht habe. Das in TUGRAZonline hochgeladene Textdokument ist mit der vorliegenden Masterarbeit identisch.

11.6.2017 ..... Datum

..... Unterschrift

STATUTORY DECLARATION

I declare that I have authored this thesis independently, that I have not used other than the declared sources / resources, and that I have explicitly marked all material which has been quoted either literally or by content from the used sources.

11.6.2017 ..... Date

..... signature

ACKNOWLEDGEMENT

The research work of this thesis was performed at the Polymer Competence Center Leoben GmbH (PCCL, Austria) within the framework of the COMET-program of the Federal Ministry for Transport, Innovation and Technology and the Federal Ministry of Science, Research and Economy with contributions by the Graz University of Technology. The PCCL is funded by the Austrian Government and the State Governments of Styria, Lower Austria and Upper Austria.

First, I would like to thank Priv.-Doz. Dipl.Chem.Univ. Dr.rer.nat. Frank Wiesbrock for the excellent supervision, professional support and educational time in his group as well as Em. Univ.-Prof. DI Dr.tech. Franz Stelzer for enabling this work.

Special thanks go to DI Franz Pirolt and Univ.-Prof. DI Dr.tech. Otto Glatter for their professional support and the good cooperation during the performance of the DLS measurements.

I am also indebted to Josefine Hobisch for the GPC measurements and the thermal analyses as well as Petra Kaschnitz for supporting me in the NMR measurements.

Sincere thanks are given to all my colleagues of the working group, especially Klaus Luef, Robin Hofmann, Martin Rausch, Zucong Zhang, Florian Mostegel and Alexander Eibel for their support and advice. Furthermore, I would like to thank all my colleagues of the ICTM for making the time at the institute to such a good time, in particular Lukas and Bettina Schafzahl, Christoph Leypold and Birgit Ehmann.

Big thanks also go to my university colleagues for the unforgettable time. I am so glad to have met you all. Thank you for supporting me, learning with me and your friendship: Josef Lechner, Lara Strohmeier, Sarah Rendl, Lukas Heupl, Hannes Kühnle, Werner Schlemmer, Ulrike Reisinger, Jakob Strasser and Rene Nauschnig. In addition to this, I would also like to thank my roommate, Sophie Radl and all my other friends and teammates who made my last 5 years such a great time, in paricular Theresa Neubauer, Janine Simon, Antonia Burger, Maria Witsch and Florian Knopper.

Finally, I want to thank my family for the strong support, always believing in me, being there for me, providing the possibility to study and the good advice in every situation. Without you, this work would not have been possible. Thanks to my parents Thomas and Renate, my sisters Johanna and Marlene and my brothers Michael and Daniel.

Table of Content

1. Introduction

The development of new drug delivery and drug targeting systems is of big interest due to their ability to minimize drug degradation and loss, to prevent side-effects and to increase the drug bioavailability and accumulation in the targeted bodily part. Several types of drug carriers exist: soluble polymers, microparticles of insoluble or biodegradable natural or synthetic polymers, microcapsules, cells, cell ghosts, lipoproteins, liposomes and micelles [1;2]. Micelles as drug carriers provide numerous advantages, such as:

- the increased bioavailability of drugs due to the micelles' ability to solubilize them
- the micelles' long term stability in small concentrations that provides gradual accumulation of the drugs in the targeted bodily parts
- their small size and variable morphology that permits accumulation in any vasculature system that, in addition, can be targeted by attachment to a specific binding site
- their stimuli-responsiveness (pH value, temperature, etc.)
- the fact that they can be comparably easily prepared in large yield
- their protection of the solubilized drug from inactivation and unfavored side-effects [3].

Amphiphilic polymers as well as low molar mass amphiphiles can be used to form micelles. However, due to their higher thermodynamic stability in comparison to low molar mass molecules, the formulation with polymers is more suitable for drug carrier systems. For the formation of micelles from polymers, non-ionic copolymers are preferably used, as the critical micelle concentration of amphiphilic ionic copolymers is very low (10^{-8} to 10^{-2} mol·L^{-1}) and, hence, polymeric micelles do not tend to disassemble upon dilution, which is an important property if they are administered intravenously [1;4]. Furthermore, the hydrophilic block of the copolymer

inherently provides the stealth effect, which extends the blood circulation time due to the adsorption of proteins from the blood [5].

As these drug delivery systems have to be introduced into an organism, several concerns must be taken into account, such as:

- the origin of the copolymer (e.g., biomaterials)
- the route of administration
- the delivered drug
- the targeted site of the drug, and
- the need of specific release.

Another important factor is the interaction between the copolymer and the biological surrounding. Therefore, the material has to be (at least) biocompatible and exhibit low or no toxicity, low to no immunogen activty, ability to solubilize drugs, and enable design flexibility with respect to size, architecture and chemical functionality [6].

Among polymeric micelles as drug carriers, copolymers of hydrophilic poly(ethylene glycol) PEG combined with another hydrophobic block have been extensively studied, due to the biocompatibility and low toxicity of PEG. However, recently published studies reported specific and non-specific recognition of PEG by the immune system. For instance, specific antibodies could be detected in the serum of patients treated with PEG-asparaginase and PEG-uricane; even in patients who never received a PEG treatment, anti-PEG antibodies were identified [7].

Disadvantages of PEG continuously trigger research for alternative (co-)polymers for biomedic(in)al applications, such as poly(2-oxazoline)s POx. POx may be referred to as bioinspired polymers regarding their biocompatibility, stealth behavior and biodistribution [7]. The *in-vitro* cytotoxicity of numerous POx-based polymers was found to be rather low in a range of cell lines [8]. The *in-vivo* toxicity of poly(2-ethyl-2-oxazoline)

PEtOx has been studied in detail yielding satisfying results [9]. In comparison with similar PEG-based systems, poly(2-methyl-2-oxazoline) PMeOx-based coatings are more stable under physiological conditions than PEG-based coatings, which show from degradation over time [10]. Antibodies against Pox-based systems have not yet been determined [6].

The polymer class of POx has many benefits, such as the numerous different monomers for the synthesis of the corresponding copolymers. Due to this variety, copolymers with tailor-made properties such as the polarity of the polymer, hydrophobic or hydrophilic behaviour, surface roughness, and/or the presence of functional groups in the side-chains for polymeranalogous modifications can be synthesized [11]. These different functional groups allow the generation of POx-based crosslinked materials via different click-chemistry reactions [12] or the incorporation of other substances into the side-chain [13].

2. Scope and Motivation

This master thesis results from a collaboration between the Polymer Competence Center Leoben PCCL and the Graz University of Technology. The motivation for this work was to investigate POx-based crosslinked micelles as potential new drug delivery systems due to the better biocompatibility of POx compared to PEG.

For the synthesis of amphiphilic block copoly(2-oxazoline)s, different monomers with respect to hydrophilicity and functional groups in the side-chain needed to be chosen. The hydrophobic block should provide an alkene function for crosslinking of the micelles via a polymeranalogous reaction like the UV-induced thiol-ene click-reaction. For crosslinking, reactants with hydrolysable bonds such as the ester bonds should be chosen. The side-chain of the hydrophilic block should be short enough for good micellization behaviour in aqueous media. A further monomer with alkyne functionality in the side-chain needed to be chosen for the incorporation of an active agent via the orthogonal synthetic strategy of the Huisgen 1,3-dipolar cycloaddition. The monomers should be synthesized from renewable resources according or be commercially available.

The block copolymerization of the monomers should be performed in a microwave reactor under autoclave conditions. For the characterization of the monomers and copolymers, IR and NMR spectroscopy as well as GPC measurements should be applied. Micelles should be prepared by the dialysis method, and the hydrodynamic radii of crosslinked, un-crosslinked and drug-loaded micelles should be determined by dynamic light scattering measurements, enabling the verification if the micelles could be crosslinked by UV-induced polymeranalogous reactions, paving the way for crosslinked micellar drug carriers that can be hydrolysed upon the application of stimuli.

3. State-of-the-Art

3.1. 2-Oxazolines

In the last decades, the polymer class of 2-oxazolines has been investigated thoroughly. Their general structure is based on a heterocyclic 5-membered ring, with the heteroatoms oxygen at position 1 and nitrogen at position 3, and a carbon atom at position 2 with a substituent (Figure 1). Due to this substituent, a large variety of monomers exists.

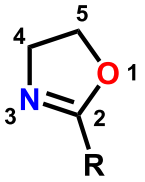

Figure 1: Structure of 2-oxazoline monomers.

3.2. Synthesis of 2-Oxazoline Monomers

Gabriel managed to successfully synthesize 2-oxazolines for the first time in 1889 [14]. These days, various synthetic strategies have been reported. For monomers with a side-chain longer than four carbon atoms, there are two very easy and commonly performed ‘one-pot’ syntheses. Carboxylic acids/esters or nitriles react with 2-aminoalcohols to form 2-oxazolines according to the Henkel patent [15] or the protocol of Witte and Seeliger [16]. In order to synthesize monomers with a shorter substituent, more complex synthesis strategies need to be applied [17, 18].

3.2.1. Synthesis of 2-Oxazolines according to Witte and Seeliger

According to Witte and Seeliger [16], nitriles react with 2-amino alcohols to yield 2-oxazolines in a one-step reaction (Scheme 1). The reaction is performed under N_2 atmosphere; as catalysts, metals salts like cadmium acetate dihydrate are used. No solvent is required for the synthesis, since the educts are liquid and molten, respectively, under the conditions applied (T > 130 °C). As side-product, ammonia gas is formed. After 25 h of stirring at 130 °C, the product can be recovered by distillation.

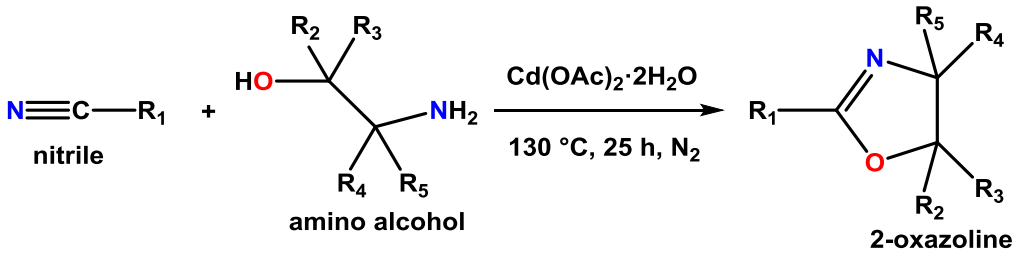

Scheme 1: Synthesis of 2-oxazolines according to Witte and Seeliger.

3.2.2. Synthesis of 2-Oxazolines via the Henkel Patent

The synthesis according to the Henkel patent [15] is a one-step reaction as well. Fatty acids react with an amino alcohol in presence of a catalyst, such as tetravalent titanium or zirconium $Zr(OR)_4$ compounds, yielding 2-alkyl- or 2-alkenyl-2-oxazolines (Scheme 2). The product is purified by vacuum distillation. As side-product, water is formed and, consequently, an inert gas atmosphere is obsolete. An additional advantage of this synthesis is the fact that the $Ti(OR)_4$ catalysts are environmentally more friendly than $Cd(OAc)_2{\cdot}2\ H_2O$ of the Witte-Seeliger synthesis. Aiming to produce 2-oxazolines in a sustainable way, it is possible to employ fatty acids from renewable resources such as undec-10-enoic acid from castor oil or decanoic acid from coconut oil. Ethanolamine can be extracted from the amino acid serine [19].

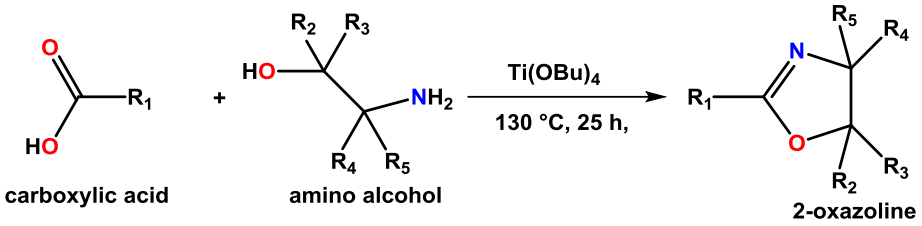

Scheme 2: Synthesis of 2-oxazolines according to the Henkel Patent.

3.2.3. Synthesis of 2-But-3'-enyl-2-oxazoline

According to Hoogenboom's synthesis strategy [18], 2-oxazolines with shorter side chains (number of carbon atoms ≤ 4) can be synthesized as follows: MeOx is added drop-wise to a freshly prepared lithium diisopropylamide LDA solution at a temperature of –78 °C under nitrogen atmosphere (Scheme 3). Afterwards, allyl bromide is added, and the reaction mixture is allowed to warm to room temperature. The mixture is stirred overnight, and then quenched with methanol. All volatiles have to evaporated under reduced pressure. The crude product is dissolved in dichloromethane DCM and is washed with water and brine. To purify the product, a vacuum distillation is performed.

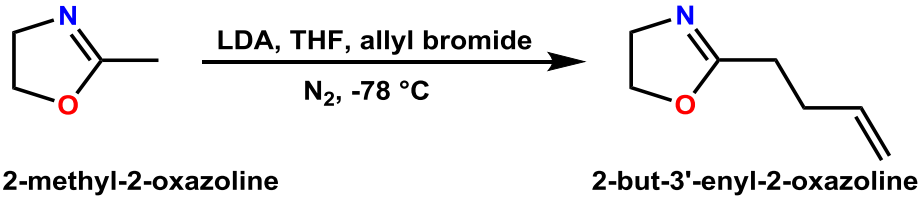

Scheme 3: Synthesis of 2-but-3'-enyl-2-oxazoline according to Hoogenboom.

The synthesis according to the protocol by Schlaad et al. [17] is a three-step synthesis. In the first step, pent-4-enoic acid is converted into an active ester. Then, chloroethylamine hydrochloride is used to form *N*-(2-chloroethyl)-pent-4-enamide. In the last step, ring-closing is performed to yield 2-but-3'-enyl-2-oxazoline (Scheme 4). This strategy has three disadvantages: long reaction times, usage of chloroform and low yields.

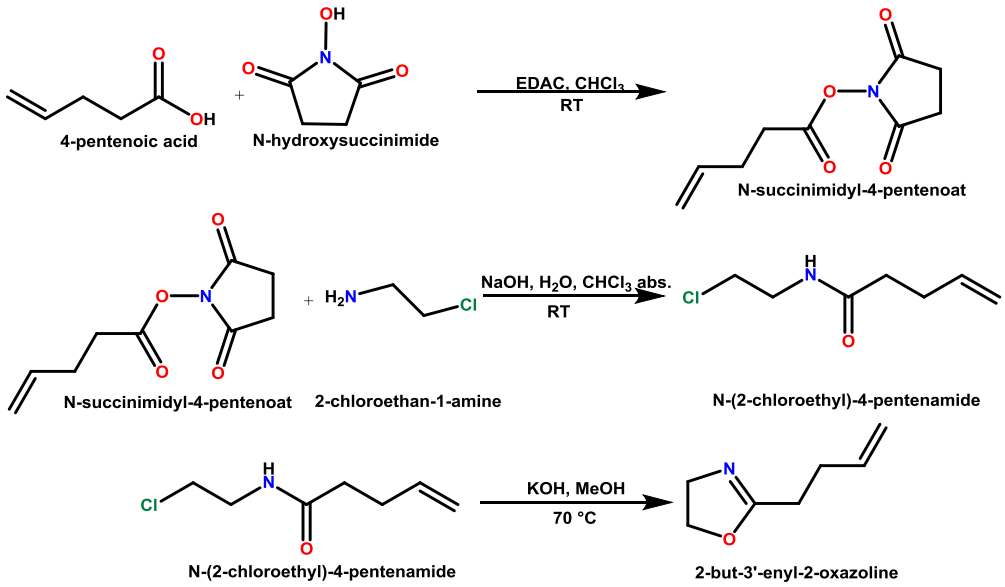

Scheme 4: Synthesis of 2-but-3'-enyl-2-oxazoline according to Schlaad.

3.3. Microwave-Assisted Polymerizations

In the 60's decade of the 20th century, four different groups discovered poly(2-oxazoline)s as a new polymer class [20-23]. The synthesis of poly(2-oxazoline)s follows a cationic ring-opening mechanism. As initiator, methyl tosylate can be used (Scheme 5) [25]. Due to the long polymerization times and the low polymerization degrees, however, this class of polymers did not play such a prominent role in the first decades after their discovery.

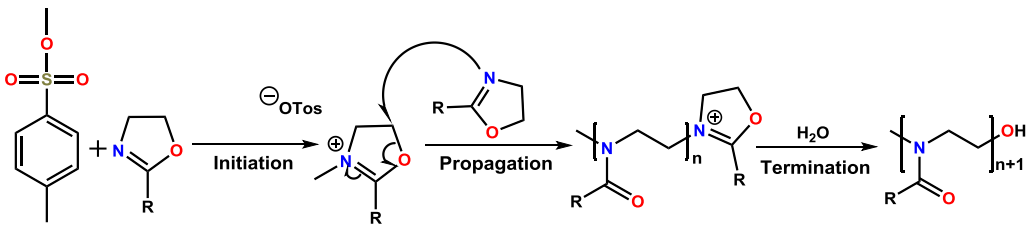

Scheme 5: Mechanism of the cationic ring-opening polymerization of 2-oxazolines with methyl tosylate as initiator.

Thanks to the development of microwave reactors for chemical synthesis, the synthesis of poly(2-oxazoline)s could be simplified, and this polymer class has been ‘re-discovered’ in the recent years [24]: Under conventional reflux conditions (e.g., at 81 °C in acetonitrile), the synthesis of PEtOx with a polymerization degree of 60 lasts 6 h. If this reaction is performed in a microwave reactor under autoclave conditions at 190 °C, it will only last 1 min. The polymerization time is reduced by the factor of 350, which correlates with the Arrhenius law. The boiling point is not a limiting factor anymore, the temperature can be increased, and the reaction is accelerated. Commonly, a temperature increase of 10 K halves the polymerization time [24].

As alternative to methyl tosylate, also alkyl nosylates and alkyl triflates can be used as initiators, which have the big advantage over halide initiators that they only propagate cationic species (and not covalent ones either) [26]. The initiation of the reaction is highly regio-selective, as recent studies of Wiesbrock et al. have shown. Due to the delocalization of the π-electrons along the N-C-O segment, the initiation of the ring-opening polymerization is initiated by a nucleophilic attack at the nitrogen atom (Scheme 5) [27]. In order to keep side-reactions like chain-transfer and chain-coupling reactions at a minimum, the polymerization should be performed in acetonitrile at 140 °C. Supplementary, under these superheated conditions, polymers with narrow average molecular weight distribution can be synthesized [25].

Due to the pseudo-living character of the ring-opening polymerization of numerous 2-oxazoline monomers, many types of (co-)poly(2-oxazoline)s are possible, like homopolymers, statistical copolymers, gradient copolymers and block copolymers [28]. Originating from the large variety of monomers with different functional groups and different lengths of the side-chains, polymers with specific properties can be synthesized [11].

3.3.1. Block Copolymerization of 2-Oxazolines

As already mentioned, it is possible to synthesize block copoly(2-oxazoline)s due to the pseudo-living character of the polymerization. Wiesbrock et al. synthesized a 4²-membered library of diblock copolymers and chain-extended homopolymers in a microwave reactor. They used 2-methyl-2-oxazoline MeOx, 2-ethyl-2-oxazoline EtOx, 2-phenyl-2-oxazoline PhOx, and 2-nonyl-2-oxazoline NonOx as monomers; each block had 50 repetition units. Aiming to achieve a polydispersity index PDI < 1.20, the order of incorporating the monomers was found to play a major role. If the monomer with the shorter side chain, like EtOx, were polymerized before the one with a larger side chain, like NonOx, a narrow molecular weight distribution could be observed. If the monomers were incorporated vice versa, the PDI was significantly higher (Figure 2) [25].

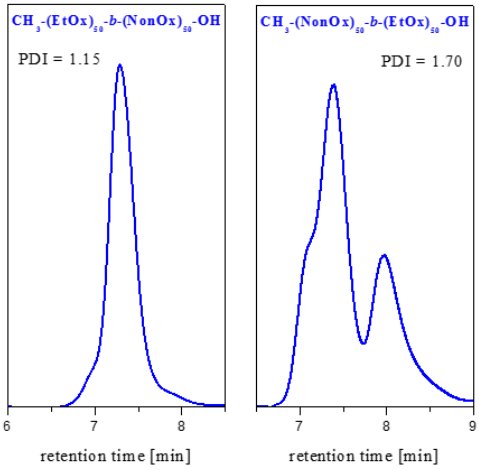

Figure 2: Influence of the incorporating order of EtOx and NonOx on the PDI of the corresponding block copoly(2-oxazoline)s [25].

These differences of the distribution of the molecular weight distribution were found to arise from chain-transfer and chain-coupling reactions, which are typical side reactions for pseudo-living cationic polymerizations [29]. The gel permeation chromatography GPC traces of the $pNonOx_{50}$-*block*-$pEtOx_{50}$ copolymer (Figure 2) reveal that a polymer fraction with higher molecular weight (shoulder at lower retention time) and a polymer fraction with lower molecular weight (signal at higher retention time) in

addition to the targeted one are formed by the side-reactions [25]. For the specific polymer pNonOx$_{50}$-*block*-pEtOx$_{50}$, the side-reactions would occur according Scheme 6:

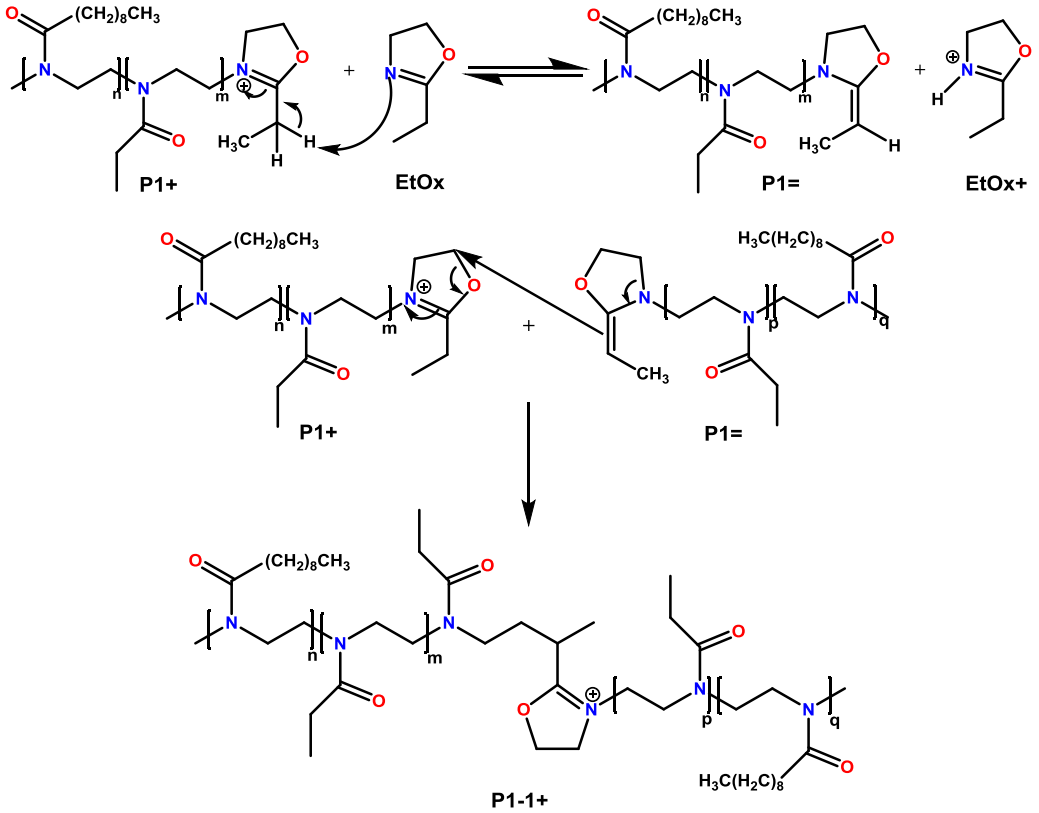

Scheme 6: Mechanism of the chain-transfer and chain-coupling reactions during the synthesis of the polymer pNonOx$_{50}$-*block*-pEtOx$_{50}$ [25].

To initiate the side-reactions, the nitrogen atom of an unreacted EtOx monomer abstracts a hydrogen atom from the α-carbon atom of the growing species **P1+**, which yields a positively charged EtOx-monomer (**EtOx+**) and an uncharged olefinic polymer **P1=**. The uncharged polymer can react, on the one hand, with **EtOx+** or, on the other hand, with another propagating polymer chain yielding **P1-1+**, which is positively charged. In summary, there are three different types of cations (**EtOx+**, **P1+** and **P1-1+**), which are able to propagate the formation of the diblock copoly(2-oxazoline) (starting from **P1+**), the high molecular weight polymer (starting from **P1-1+**), and the low molecular weight polymer (starting from **EtOx+**) [25].

Thermogravimetric analyses of the block copoly(2-oxazoline) library of Wiesbrock and his colleagues showed that all copolymers were stable to temperatures of approx. 300 °C. Their glass-transition temperatures T_g ranged from 57 to 107 °C. Copolymers that included at least one block of pNonO did not have a measurable T_g [25]. In general, the glass transition temperature decreased with the number of atoms in the side-chain [30]. In further studies, also the mechanical properties, particularly the E-moduli, of these block copolymers were determined [31]. Other studies revealed the correlation between the arrangement of blocks in copoly(2-oxazoline)s and their micellization behavior, which will be discussed in chapter 3.5.3.

3.3.2. Statistical Copolymerization of 2-Oxazolines

Statistical copoly(2-oxazoline)s have a random arrangement of repetition units. Monomers with similar polymerization rates form randomly ordered copolymer chains. Schubert and his group compared statistical and block copoly(2-oxazoline)s composed of EtOx and NonOx. Their molecular weight distribution, kinetics and surface energy were determined [32]. The contact angle measurements showed that the surface energy is reduced with increasing content of NonOx side-chains on the surface of a polymer film. In comparison with diblock copolymers, this effect is reduced for statistical copolymers [33, 34]. Furthermore, statistical copolymers have a lower degree of crystallinity and a lower T_g. Their E-moduli are lower, and the creep compliance and mechanical energy dissipation are higher. The surface energy is strongly influenced by the mobility of the side-chain [35].

Homopolymers and amorphous copoly(2-oxazoline)s of EtOx and 2-(3'-ethylheptyl)-2-oxazoline EHOx were synthesized by Schubert and colleagues [36]. The ratio EtOx:EHOx was varied from 100:0 to 0:100, and the surface energies and thermal properties of the POx were determined. A linear dependency between the EHOx amount in the copolymers and

the glass transition temperature could be observed. Increasing the amount of EHOx results in a decrease of the surface energy; additionally, the branching position strongly influences the side chain mobility [35]. In further studies, statistical copolymers from monomers with unsaturated side chains, like “SoyOx”, a 2-oxazoline monomer based on fatty acids of soya, were produced [37]. Copolymers based on 2-oxazolines and 2-oxazines were also synthesized. Here, an increasing steric hindrance results in low polymerization rates [38].

3.3.3. Gradient Copolymerization of 2-Oxazolines

For gradient copolymerizations, monomers with different polymerization rates have to be used. Hoogenboom, Schubert and colleagues polymerized combinations of MeOx, EtOx, NonOx, and PhOx [39]. Due to the slow polymerization of PhOx, gradient-statistical, gradient-block, and statistical-block polymers could be synthesized in one step [40].

3.4. Polymeranalogous Reactions of Poly(2-oxazolines)

There are numerous polymeranalogous reactions to modify copoly(2-oxazolines) and change the functionalities of their side chains and properties. One class of polymeranalogous reactions are the so called click-reactions. Click-chemistry has many advantages, such as

- no dangerous side-products
- high selectivity
- regio- and stereospecificity
- nearly quantitative conversion

- mild reaction conditions
- water as solvent (whenever possible)
- orthogonality to other organic reactions
- insensitivity to moisture and oxygen, and
- a large variety of educts [41].

In this chapter, two different click-reactions, the thiol-ene click-reaction and the Huisgen 1,3-dipolar cycloaddition, will be described.

3.4.1. Thiol-Ene Click-Reactions

Generally, two common thiol-ene click reactions exist: the radically initiated addition of a thiol to an electron-poor or electron-rich carbon-carbon bond, as well as the thiol-Michael-addition to electron-poor carbon-carbon bonds. Since the reaction can be carried out under mild conditions and has a broad variety and is highly efficient, it is often used to crosslink polymer networks [12]. The radical thiol-ene reaction can be initiated thermally or by UV-light irradiation [41]. To initiate the reaction by UV light, a small amount of photoinitiator PI (e.g., Irgacure® TPO-L) is required. The PI dissociates homolytically into two radical fragments, which interact with the thiol to yield a thiyl radical (Scheme 7).

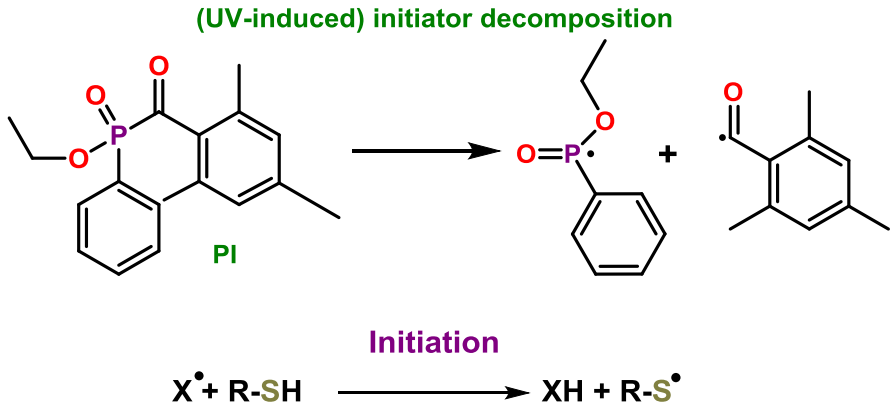

Scheme 7: Initiation of the thiol-ene click-reaction by by UV-induced decomposition of the photoinitiator PI.

These thiyl radicals react with olefinic double bonds to yield thioethers. The thiol-thiyl cycle (Scheme 8) is one of the main characteristics of the thiol-ene reaction and exhibits only a few side-reactions (like thiyl-thiyl dimerizations) [42].

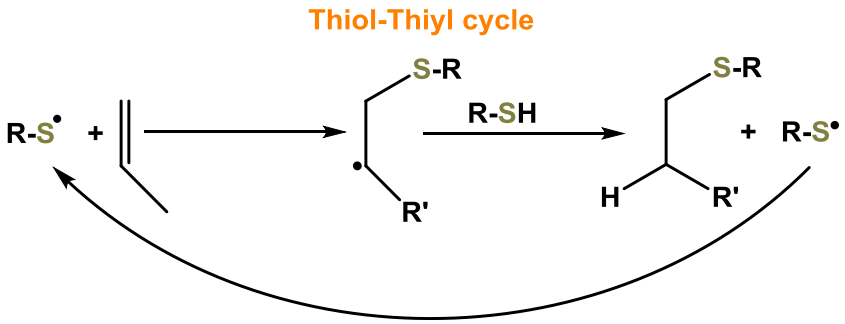

Scheme 8: Reaction scheme of the thiol-thiyl cycle.

3.4.2. Poly(2-oxazoline)s Functionalized by Thiol-ene Click-Reactions

Olefinic side-chains of poly(2-oxazoline)s can be functionalized by the thiol-ene reaction. Gress, Völkel and Schlaad reacted poly[2-(but-3'-enyl)-2-oxazoline] pBu$^{=}$Ox and methyl-3-mercaptopropionate [43]. Schubert and his group synthesized copoly(2-oxazoline)s with varied concentrations of the monomers EtOx and 2-dec-9'-enyl-2-oxazoline Dec$^{=}$Ox (unsaturated double bond between C9 and C10). The repetition units of Dec$^{=}$Ox were functionalized by the thiol-ene reaction with fluorescein enabling to investigate the cellular uptake of these copoly(2-oxazoline)s, the particle size of which varied from 200 to 600 nm [44].

Furthermore, it is possible to produce copoly(2-oxazoline)-based three-dimensional frameworks by means of UV-induced thiol-ene reactions. In different studies, the swelling capacity of crosslinked poly(2-oxazoline)-based networks was observed [45-48]. Due to the biodegradability of this polymer class, poly(2-oxazoline)-based hydrogels were investigated for medical and medicinal technologies [49]. Wiesbrock et al. reported the

adhesion of cancer cells to peptides bound to the hydrogels; in a further study, they evaluated the enzymatic degradation of hydrogels at different pH values [46]. Crosslinked poly(2-oxazoline)s are also utilized as photoresists [19;50;51] or as antireflective coatings [13] and, in addition, crosslinked pNonOx$_{80}$-*stat*-pDec$^{=}$Ox$_{20}$ copolymers could be used an alternative to polyamides for high-voltage insulators due to their electrical conductivity and permittivity [52].

3.4.3. Huisgen 1,3 - Dipolar Cycloaddition

Via the Huisgen 1,3-dipolar cycloaddition of azides and alkynes, 1,2,3-triazoles can be synthesized, which are relatively stable under various conditions. Azides and alkynes are not affected by highly functionalized biological molecules, molecular oxygen, water, numerous reaction conditions of organic synthesis [53;54] and subsequent transformations [55]. However, azides could decompose with exothermal release of nitrogen [56]. In spite of the thermodynamically favored decomposition of azides, other kinetic factors make aliphatic azides nearly indiscernible until a good dipolarophile is present [54]. The high kinetic stability of azides and alkynes results in their slow cycloaddition, which needs high temperatures and long reaction times [57;58]. In absence of a catalyst, only coupling reactions with highly electron-deficient terminal alkynes are regioselective [59]; otherwise, a mixture of 1,4- and 1,5-regioisomers is obtained (Scheme 9) [57].

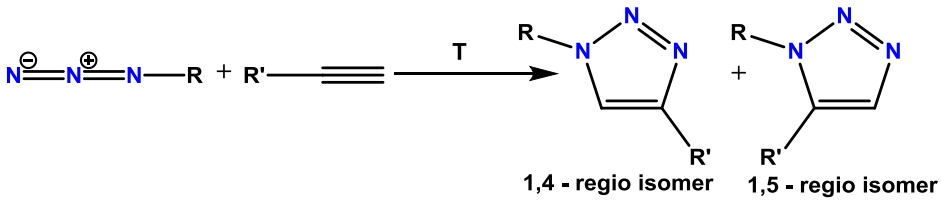

Scheme 9: Uncatalyzed Huisgen 1,3-dipolar cycloaddition.

The use of a Cu(I)-catalyst improves the regioselectivity, and only the 1,4-regioisomer is obtained (Scheme 10), while the reaction rate is increased to 10^7 times without employment of high temperatures [60]. High yields can be achieved, and numerous functional groups are tolerated, without long and complicated work-up and purification [54;61]. The reaction can be performed in various solvents, at a wide range of pH values and temperatures. As Cu(I)-catalyst, copper-iodide or Cu(II)-salts, which are in-situ reduced to Cu(I), can be used (Scheme 11) [56].

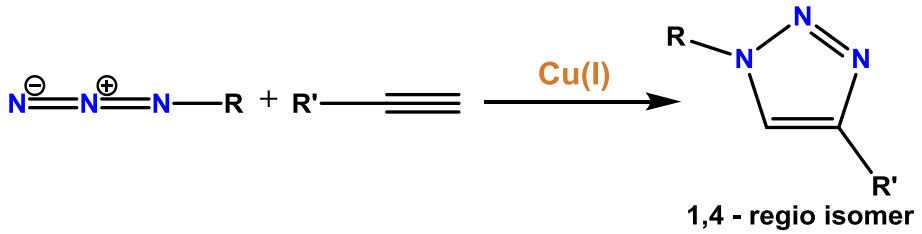

Scheme 10: Cu(I)-catalyzed Huisgen 1,3-dipolar cycloaddition.

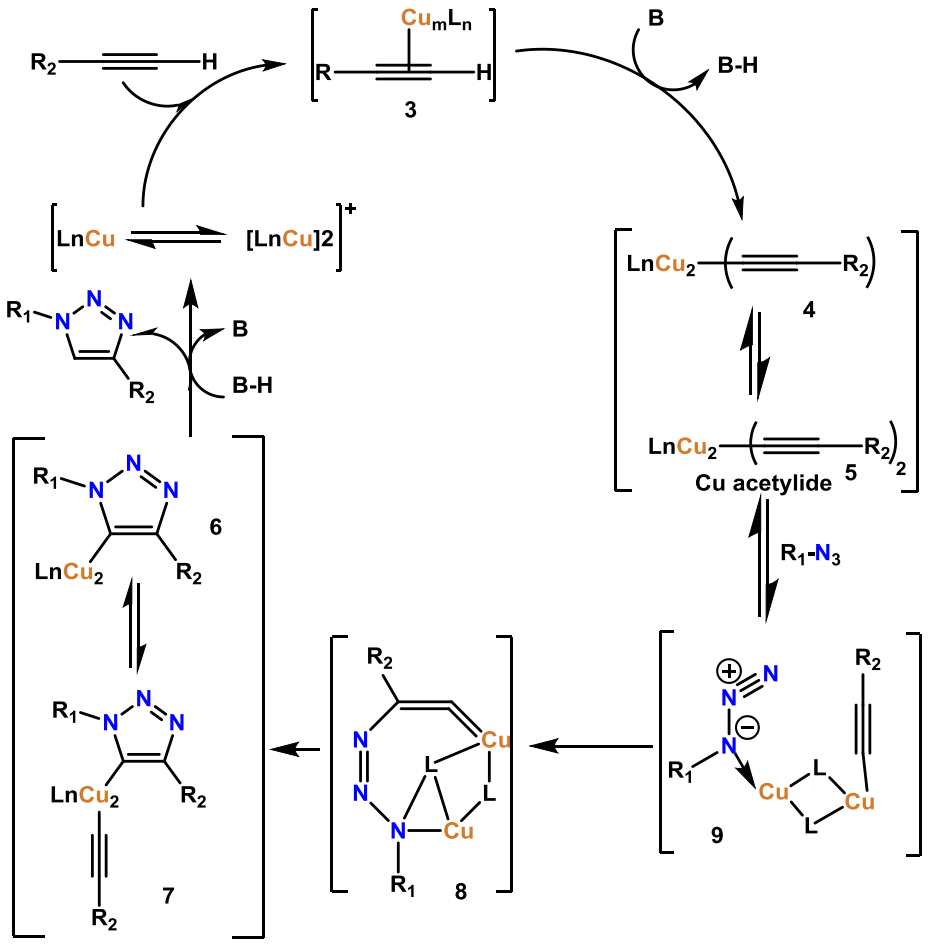

Scheme 11: Reaction mechanism of the Cu(I)-catalyzed Huisgen 1,3-dipolar cycloaddition.

The coordination of the alkyne decreases its pK_s value, and the coordination of the azide activates it for the nucleophilic attack. The N3-atom attacks the C4-atom in nucleophilic fashion, and a metallocycle is generated. The azide is positioned in the metallocycle for further ring contraction by transannular interaction between the lone pair of N1 and the C5-atom. The metallocycle transforms relatively fast into the triazole-copper derivate, which is protonated by interaction with an external base or solvent molecule. After dissociation of the product, the reaction ends and the catalyst can be regenerated [62]. The strong dipolar moment of the triazole ring can form hydrogen-bonds and increases the hydrophilicity, while it is stable under biological conditions [63].

3.4.4. Modification of Poly(2-oxazoline)s via the Huisgen 1,3-Dipolar Cycloaddition

MeOx, EtOx, and 2-pent-4'ynyl-2-oxazoline Pen$^{\equiv}$Ox were copolymerized by Jordan and co-workers. The cycloaddition of azides onto the side-chains of Pen$^{\equiv}$Ox yielded triazoles [63]. Alkyne-functionalized poly(2-oxazoline)s, namely pMeOx-*stat*-pPen$^{\equiv}$Ox and pEtOx-*stat*-pPen$^{\equiv}$Ox, were reacted with icosahedral virus-like particles having an azide-functionalized surface [65]. Different poly(2-oxazoline)s were functionalized with an alkyne-group in the backbone by the group of Schubert, and the applicability of the functionalized polymers for click-chemistry was evaluated with different azides like heptakis(azido-b-cyclodextrin) [66]. Cortez and Grayson fixed terminal azides at an end of poly(2-ethyl-2-oxazoline) for preparing star polymers, diblock copolymers and cyclic polymers [67]. Volet et al. synthesized poly(2-oxazoline)s with di-terminal azido functions to conjugate various ligands with an alkyne group by 1,3-cycloaddition [68]. Triazole-linked poly(ε-caprolactone)-*graft*-poly(2-methyl-2-oxazoline) copolymers as potential drug delivery systems were synthesized and evaluated by Guillerm and co-workers [69].

3.5. Micelles

3.5.1. General Aspects

Micelles are colloidal dispersions, consisting of a dispersed phase distributed within a continuous phase. Normally, colloidal dispersions are greater than molecular dispersions (particle size < 1 nm) and smaller than coarse dispersion (particle size > 0.5 µm). Colloidal dispersions can be divided in three groups: lyophilic, lyophobic and association colloids. Micelles belong to the so-called association or amphiphilic colloids. At specific conditions (temperature and concentration), amphiphilic or surface active agents, e.g. molecules consisting of two regions with opposite affinities to a given solvent, can form micelles spontaneously [70].

In a solvent at low concentration, amphiphilic molecules are separated; if their concentration increases, they start to aggregate within a narrow concentration interval (Figure 3). The major driving force is the decrease of free energy of the system due to the protection of the hydrophobic part from water by hydrophilic fragments [71].

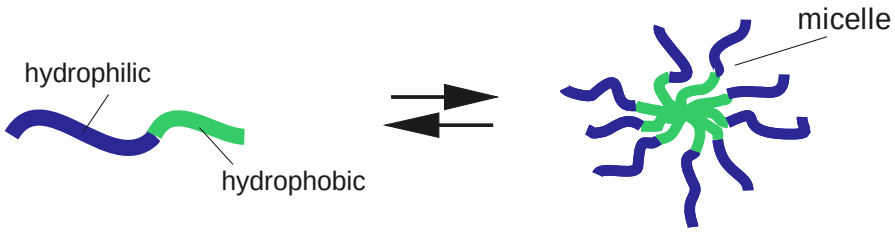

Figure 3: General scheme of micelle formation.

A large number of amphiphilic molecules are required to form a micelle, which can occur in different shapes, like spherical (most common), rod-like, worm-like, globular, disk-like or as vesicle or bilayer [72, 73]. One important property of micelles is their ability to increase the solubility of insoluble substances, due to their anisotropic water distribution within the structure. The water concentration decreases from the hydrophilic corona

to the hydrophobic core. This phenomenon results in a polarity gradient, which influences the position of a substance within the micelle. In an aqueous system, a non-polar substance will be aggregated inside the core of the micelle, while polar substances will be adsorbed at the surface of the micelle. Medium polar substances will be distributed along the surfactant molecules at specific intermediate positions (Figure 4). The micelle's capacity depends on many factors, like the structure of the drug and the surfactant, their polarities, the location of the drug within the micelle, temperature, pH-value, etc. [74].

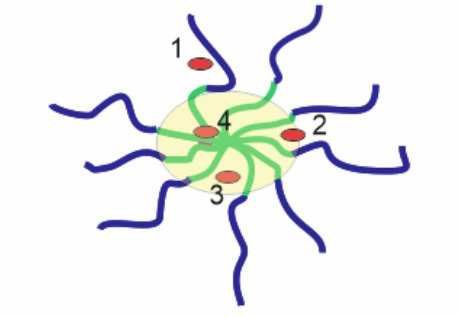

Figure 4: Possible positions of a drug within the micelle, depending on polarity. 1: completely hydrophilic particle in corona; 2/3: intermediate polarity of the particle; 4: completely hydrophobic particle within the core.

Micelles formed by polymers represent a class of their own. The copolymers need to be composed of hydrophilic and hydrophobic monomer units. The most important classes of polymers and copolymers are represented in Figure 5: Homopolymers consist of only one type of monomers, so they cannot form micelles. Copolymers have at least two types of monomers with different solubility. The organization of the different monomers provides different types of copolymers [75]. Commonly, copolymers with a larger hydrophilic than hydrophobic part can form spherical micelles in water. They are consisting of a hydrophobic core and a hydrophilic corona. If the hydrophilic block is too long, copolymers may occur as unimers in water; otherwise, if the hydrophobic block is too long, they form rod- and worm-like as well as lamellae structures [75]. Such micelles are bigger than spherical micelles and, hence, they do not delay clearance by macrophages of the liver and spleen by parental administration, which enables their accumulation in the

targeted regions (e.g., bodily parts) and controlled drug-release. The drug-loading capacity of worm-like micelles is higher, and they are able to persist up to one week *in-vivo* in the blood circulation. Worm-like structures are formed due to the hydration and swelling of the corona [76].

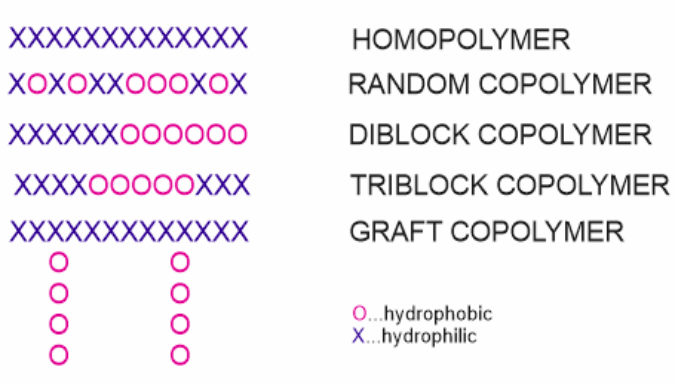

Figure 5: Structural types of copolymers.

Generally, the core of a micelle has a molten liquid nature, which allows effective mixing of the hydrophobic fragments and results in a thermodynamic quasi-equilibrium state. Diluting can shift the micelle:unimer equilibrium in the direction of the unimers, and can cause dissociation of the micelles. At concentrations above the critical micelle concentration CMC, micelles should be long-term stable [1;77].

There are two main types of micelle preparation methods, the direct dissolution method and the dialysis method [78]. The choice of the method is dependent on the solubility of the micelle-forming block copolymers in water. For copolymers with limited solubility in water, the direct dissolution method can be used. The copolymer is simply dissolved in an aqueous medium above its CMC at room or elevated temperature. Copolymers with very low solubility in water can be converted into micelles by the dialysis method. They are dissolved in a water-miscible organic solvent (dimethylsulfoxide, acetonitrile, tetrahydrofuran, acetone…) and subsequently dialyzed against water.

Eisenberg and co-workers have shown in numerous studies that block copolymer micelles can exist in various different morphologies: spheres, different kinds of rods and vesicles, tubules, branched tubules, baroclinic tubes, needles, large compound micelles, lamellae, hexagonally packed hollow hoops, various mixed and combined morphologies, etc. [75;78-83]. Different morphologies can be observed at equilibrium, near-equilibrium and non-equilibrium conditions. Generally, non-spherical micelles are formed by asymmetric block copolymers, in which the length of the hydrophobic block is significantly shorter than the length of the hydrophilic one. The composition of the copolymer (degree of stretching of hydrophobic blocks and the interaction between hydrophilic blocks), the concentration of the copolymer (aggregation number), and the type of organic solvent used are the key factors for different morphologies [78].

3.5.2. Influence of Temperature and Concentration on the Formation of Micelles

The (minimum) unimer concentration required to form micelles is the so-called critical micelle concentration CMC. The number of individual molecules that form a micelle is the so-called aggregation number [1]. At concentrations near the CMC, micelles are not close-packed and contain some water in the core [84]. With increasing concentrations of the amphiphile, the unimer:micelle equilibrium shifts toward micelles, which become more tightly packed, stable and smaller, since the residual solvent is removed from the core.

The lower the CMC of an amphiphile, the more stable the micelles are. This trend is particularly important for the usage of micelles as drug delivery systems, since they have to be stable upon dilution within a large volume of blood. Micelles with low CMC will be stable; micelles with high CMC, however, easily dissociate into unimers, and drugs occluded in their core might precipitate in the blood [85].

Micellization is affected by numerous factors, like temperature, solvent, additives, pressure, pH-value, ionic strength, and unimer nature (chain length, hydrophobic volume, head group area, etc.) Consequently, the CMC varies upon changing the environmental conditions [86]. In general, the CMC decreases with increasing temperature, due to destruction of hydrogen bonds between water molecules and the hydrophilic block; log(CMC) depends (nearly) linear on the inverted temperature T^{-1} [87].

Studies for amphiphilic PEG-based copolymers have shown a local minimum in the CMC-temperature curve at approx. 50 °C, which is shifted to higher temperatures with increasing PEG content [88]. The initial decrease is caused by the smaller probability of hydrogen bond formation at increasing temperature, concomitant with decreasing hydrophilicity of the molecule. Therefore, micellization occurs at lower concentrations. However, further increase of the temperature renders the effect of the hydrophobic blocks more dominant, which disfavors micellization, and the CMC increases with higher temperature after reaching the minimum [89].

To determine the CMC, different methods can be applied. One method is to measure the changes in surface tension by increasing the amount of the amphiphiles. Amphiphilic molecules tend to be adsorbed at the air-water interface below the CMC. Hence, increased concentrations of amphiphilic molecules result in saturation of interface and bulk of the solvent (water) with amphiphiles. This point corresponds to the CMC, and any further increase in concentration of amphiphilic unimers triggers the formation of micelles in the bulk phase and a decreasing free energy of the system. Below the CMC, a decreasing surface tension with increasing amphiphile concentration can be observed; above the CMC, the surface tension stays constant with increasing concentration, which is an evidence for saturation of the interface [74].

Furthermore, HPLC, small-angle light scattering and fluorescent spectroscopy can be used to determine the CMC [90, 91]. Fluorescent spectroscopy is based on the preferred association of fluorescent probes, like pyrene, with micelles rather than with water. Their fluorescence depends on the surrounding. Below the CMC, only a small amount of pyrene is solubilized in water (polar solvent), but with increasing micelle concentration, the solubility of pyrene is increased (hydrophobic core of the micelles). This can be observed by increasing fluorescence intensities, if the concentration of an amphiphilic polymer reaches the CMC and micelles begin to appear [71].

The critical micellization temperature CMT is another important parameter to describe the formation of micelles. Below the CMT, only unimers exist. Above the CMT, unimers and micelles are coexisting in the system. In order to determine the CMT, the same methods can be applied that are used to quantify the CMC. CMC, CMT and their dependence on temperature and concentration can be used for calculations of thermodynamic parameters of micellization, like free energy and enthalpy of the formation of micelles [1].

3.5.3. Self-Assembly of Block Copoly(2-oxazoline)s

The group of Sato synthesized amphiphilic diblock copoly(2-oxazoline)s that form core-shell micelles in water at 50 °C. The micelles formed big concentrated phase droplets by further aggregation, and bulk phase separation occurred due to droplet coalescence. At 70 °C, there was no coalescence of the hydrophilic (pEtOx) blocks into a liquid bulk phase observable, due to the sufficient hydrophobicity of the blocks [92].

The solution behavior of double-hydrophilic PEG-*block*-pMeOx was studied by Schlaad's and Taubert's groups. The presence of aggregates could be confirmed by pulsed-field gradient NMR spectroscopy [93].

Hoogenboom, Kjoniksen et al. synthesized pEtOx-*block*-p(EtOx-*stat*-PrOx) copolymers and observed a similar aggregation behavior. The block copoly(2-oxazoline)s featured two cloud points upon heating. At the first cloud point, aggregates formed and fragmented into smaller structures like micelles. If the temperature increased, double hydrophobic behavior was observed, and large compact aggregates were formed [94].

Micelle formation of numerous pNonOx-*block*-pEtOx copolymers on surfaces during spin-coating was observed by Gohy and co-workers. If the solvent evaporates, the more hydrophobic pNonOx part precipitates. Size and structure of the micelles varied with content of pNonOx [95].

Jordan, Papadakis et al. synthesized amphiphilic and fluorophilic diblock copoly(2-oxazoline)s. In aqueous media, the amphiphilic copolymers formed spherical micelles, and the fluorophilic copolymers elongated assemblies. Intermixing could not be observed, but those micelles coexisted [96]. The introduction of phosphine ligands into amphiphilic block copolymers based on poly(2-oxazoline)s by polymeranalogous P-C coupling between side-chains with aryliodide and bisaryl phosphine was investigated by Nuyken and his group. High catalytic activity of the micellar catalysts could be obtained [97].

Schubert et al. investigated the formation of spherical micelles with a pEtOx corona and a pSoyOx core in aqueous solution. The core could be crosslinked by UV-irradiation, so a solvent change from water to acetone results in short, rod-like micelles, due to the swelling of the core. This effect is useful for the deposition and the release of molecules [98].

Other studies figured out a correlation between the arrangement of blocks in copoly(2-oxazoline)s and their micellization behavior. Micelles with a hydrophobic block in the middle are smaller than those with a hydrophilic

block in the center. For those studies, triblock copoly(2-oxazoline)s [99] and tetrablock copoly(2-oxazoline)s [100] were synthesized. Jordan, Papadakis et al. reported the aggregation behavior of di- and triblock copoly(2-oxazoline)s, and they also claimed that the architecture of the micelles correlated with the composition of the copolymers [101].

Schubert and his group synthesized diblock copoly(2-oxazoline)s to form micelles for the thermoreversible phase transfer between hydrophobic ionic liquids and water [102], and triblock amphiphilic/fluorophilic copolymers, where two T_gs could be detected, which is an indication for the immiscibility of blocks in the copoly(2-oxazoline)s [103]. Di- and triblock copoly(2-oxazoline)s were also synthesized by Kabanov and co-workers to solubilize water-insoluble drugs like Paclitaxel®. Excellent drug loading efficiencies could be observed [104].

Montemagno et al. produced amphiphilic triblock copoly(2-oxazoline)s by using a telechelic macroinitiator for the ring-opening polymerization of EtOx. The triblock copolymers formed vesicles in water [105]. The preparation of block copolymers containing blocks of 2-oxazoline derivatives with *N*-heterocyclic caben/palladium catalysts in the hydrophobic part was described by Weberskirch and co-workers. The amphiphilic block copolymers self-assembled in aqueous solution and were used for Heck and Suzuki coupling reactions [106;107]. The formation of triblock copoly(2-oxazoline)-based micelles and their loading with numerous hydrophobic anticancer agents was investigated by Kabanov, Luxenhofer et al. The stability of the multidrug-loaded micelles was higher compared to single-drug loaded micelles, and very effective against several tumor models [108].

4. Results and Discussion

2-Oxazoline monomers, a crosslinker, and a model drug needed to be chosen for the synthesis of amphiphilic block copoly(2-oxazoline)s and the preparation and characterization of drug-loaded crosslinked micelles thereof.

- As hydrophilic monomer, commercially available and water-soluble 2-ethyl-2-oxazoline EtOx was chosen.
- 2-Dec-9'-enyl-2-oxazoline Dec$^{=}$Ox was selected as hydrophobic monomer. It can be synthesized from renewable resources according the Henkel patent [15] and contains olefinic side-chains enabling crosslinking by polymeranalogous thiol-ene reactions.
- As thiol compound for the crosslinking reactions, bisfunctional glycol dimercapto acetate GDMA was chosen, which contains hydrolysable ester bonds.
- The commercially available monomer 2-(pent-4-ynyl)-2-oxazoline Pen$^{\equiv}$Ox was chosen due to its alkyne function in the side-chain as third monomer for the covalent attachment of azide-functionalized drugs.
- Finally, pharmaceutically active compound Zidovudine bearing an azide group was chosen as model drug.

The block copolymerizations yielding either pEtOx-*block*-pDec$^{=}$Ox or pEtOx-*block*-p(Dec$^{=}$Ox-*stat*-Pen$^{\equiv}$Ox) copolymers were performed in a microwave reactor. Via the Huisgen 1,3-cycloaddition, Zidovudine was connected to the triblock copolymer. According the dialysis method, micelles were formed and crosslinked by the thiol-ene click reaction with GDMA. The hydrodynamic radii of the micelles were analyzed by dynamic light scattering measurements, and the CMC was determined by measuring the surface tension in dependency on the concentration.

4.1. Synthesis of Dec$^{=}$Ox

Dec$^{=}$Ox was synthesized according to the Henkel patent [15] from the fatty acid 10-undecenoic acid from castor oil and ethanolamine, with $Ti(OBu)_4$ as catalyst (Scheme 12).

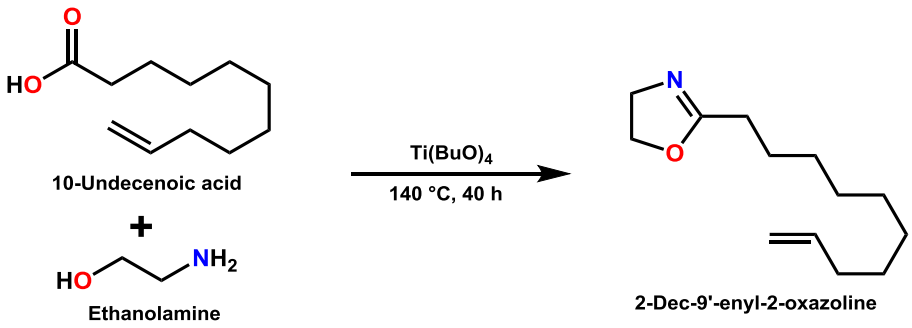

Scheme 12: Synthesis of 2-Dec-9'-enyl-2-oxazoline.

The monomer was purified by vacuum distillation from the reaction mixture. Dec$^{=}$Ox was obtained in high purity and yield (Figure 6).

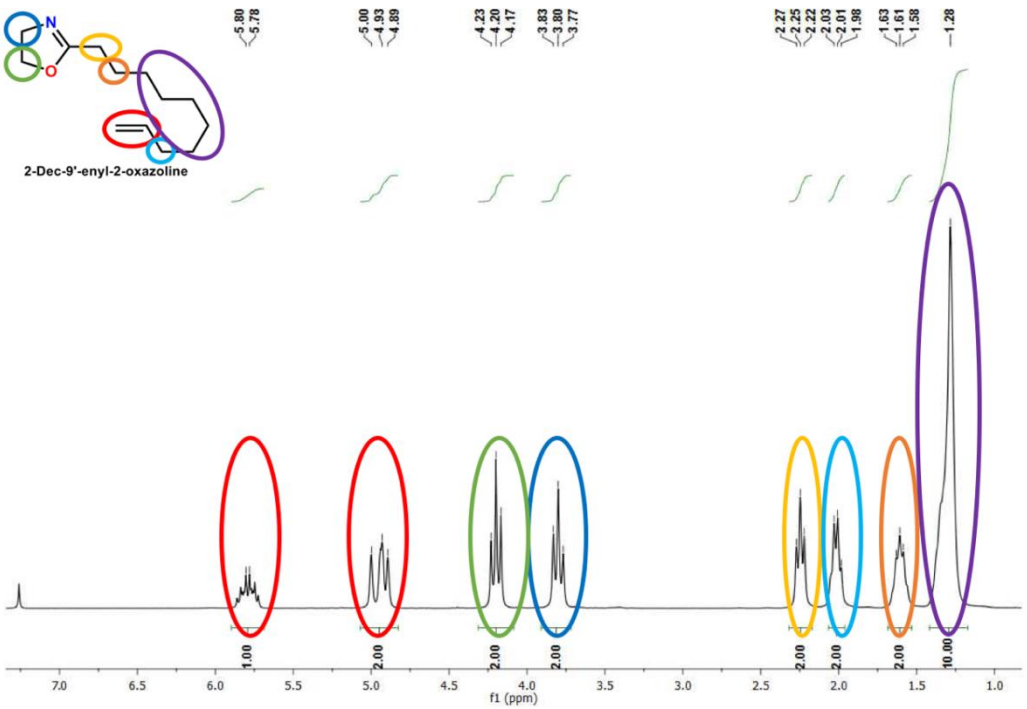

Figure 6: ^{1}H-NMR spectrum of Dec$^{=}$Ox.

4.2. Synthesis of Block Copoly(2-oxazoline)s

Via the microwave-assisted, pseudo-living cationic ring-opening polymerization of EtOx, Dec$^{=}$Ox, and Pen$^{=}$Ox, block copolymers of the targeted compositions can be synthesized. All synthesis were performed on the 2 g scale (amount of the copoly(2-oxazoline)s). The hydrophilic block was synthesized first (see chapter 3.3.1). Hydrophilic EtOx (and eventually Pen$^{=}$Ox) was/were weighed into a dry and argon-flushed 5 mL microwave vial, and the initiator methyl tosylate and the solvent acetonitrile were added. The polymerization of the first block was performed under autoclave conditions in a Biotage microwave reactor at 140 °C and 4 bar for 1 h. Afterwards, the hydrophobic monomer Dec$^{=}$Ox and additional acetonitrile were added under inert conditions, and the polymerization of the second block was performed at 140 °C and 4 bar for 1 h. After removal of the solvent, the copolymer was dried under reduced pressure (< 2 mbar) for 1 d.

4.2.1. pEtOx$_{95}$-*block*-pDec$^{=}$Ox$_5$

The ^{1}H-NMR spectrum of pEtOx$_{95}$-*block*-pDec$^{=}$Ox$_5$ (Figure 7) reveals the absence of any residual monomers. Furthermore, it allows to verify the 95:5 ratio of the repetition units: Assuming that the polymer back-bone has 400 (= 100·4) hydrogen atoms, the methyl end group of the EtOx side-chain shows 285 (= 95·3) hydrogen atoms, and the double bond at the end of the Dec$^{=}$Ox side-chain has 10 (= 5·2) hydrogen atoms. The small signals, next to the solvent ($CDCl_3$) originate from toluene sulfonic acid, formed by the initiator upon work-up. GPC measurements of the first block and the whole polymer were performed with $CHCl_3$/Et_3N/^{iso}PrOH (94/4/2) as eluent. The small shift to shorter retention times for the copolymer is indicative of higher molecular weight in comparison to the homopolymer (Figure 8). The determined PDI is 1.4.

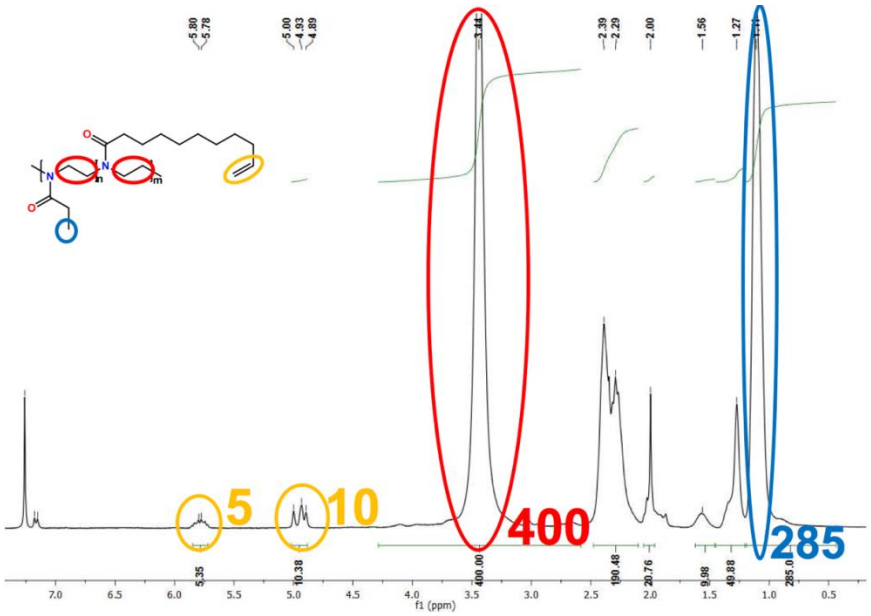

Figure 7: ^{1}H-NMR spectrum of the block copolymer pEtOx$_{95}$-*block*-pDecOx$_{5}$.

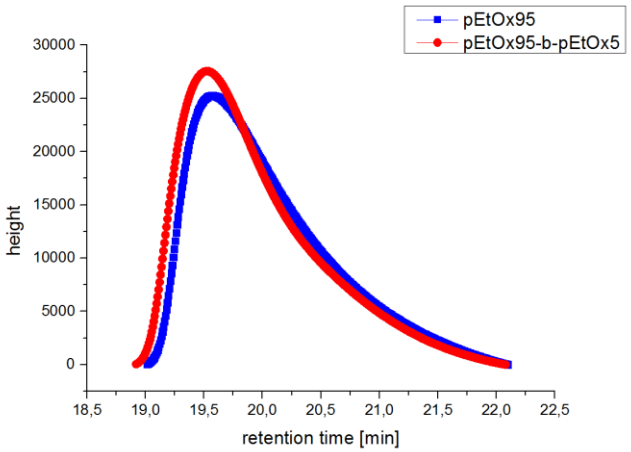

Figure 8: Size-exclusion chromatogram of pEtOx$_{95}$-*block*-pDecOx$_{5}$.

4.2.2. pEtOx$_{90}$-*block*-pDec$^{=}$Ox$_{10}$

The ^{1}H-NMR spectrum of pEtOx$_{90}$-*block*-pDec$^{=}$Ox$_{10}$ (Figure 9) also reveals the absence of any residual monomers; the 90:10 ratio of the repetition units could be verified (polymer back-bone: 400 (= 100·4), methyl groups of pEtOx: 270 (= 90·3), and double bonds of pDec$^{=}$Ox: 20 (= 10·2) hydrogen atoms). The GPC of the copolymer reveals shorter retention times in comparison to the homopolymer (Figure 10); PDI = 1.5.

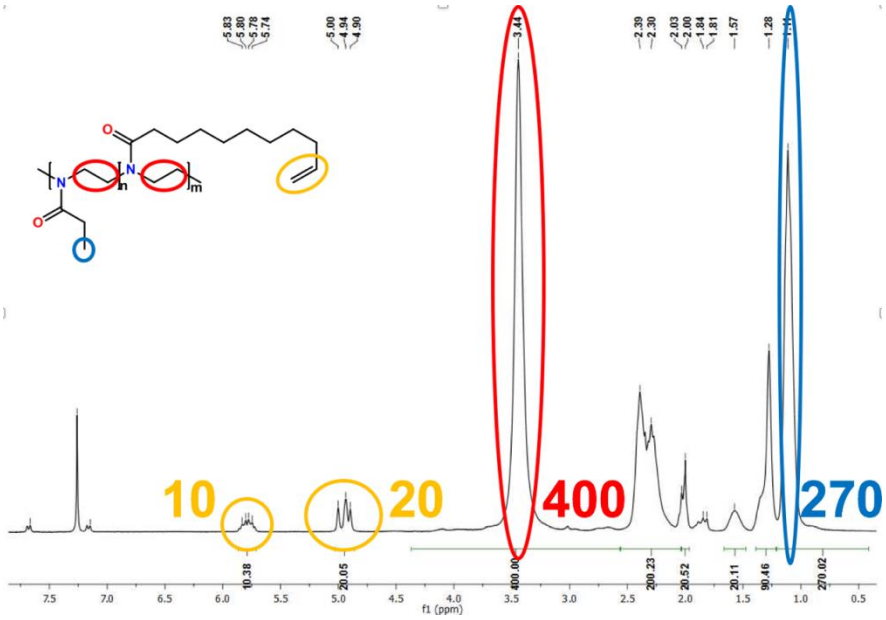

Figure 9: ^{1}H-NMR spectrum of pEtOx$_{90}$-*block*-pDec$^{=}$Ox$_{10}$.

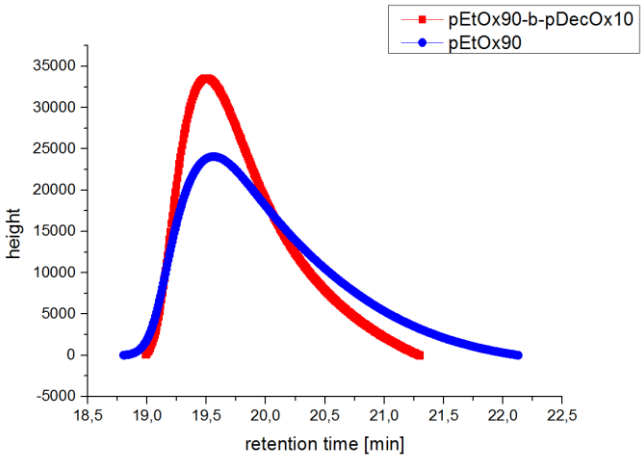

Figure 10: GPC measurement of pEtOx$_{90}$-*block*-pDec$^{=}$Ox$_{10}$.

4.2.3. pEtOx$_{85}$-*block*-pDec$^{=}$Ox$_{15}$

The ^{1}H-NMR spectrum of pEtOx$_{85}$-*block*-pDec$^{=}$Ox$_{15}$ (Figure 11) again reveals the absence of any residual monomers and enables to verify the 85:15 ratio of the repetition units (polymer back-bone: 400 (= 100·4), methyl groups of pEtOx: 255 (= 85·3), and double bonds of pDec$^{=}$Ox: 30 (= 10·3) hydrogen atoms). Once again, GPC measurements reveal a higher molecular weight of the copolymer than the homopolymer (Figure 12) a PDI of 1.4 was measured.

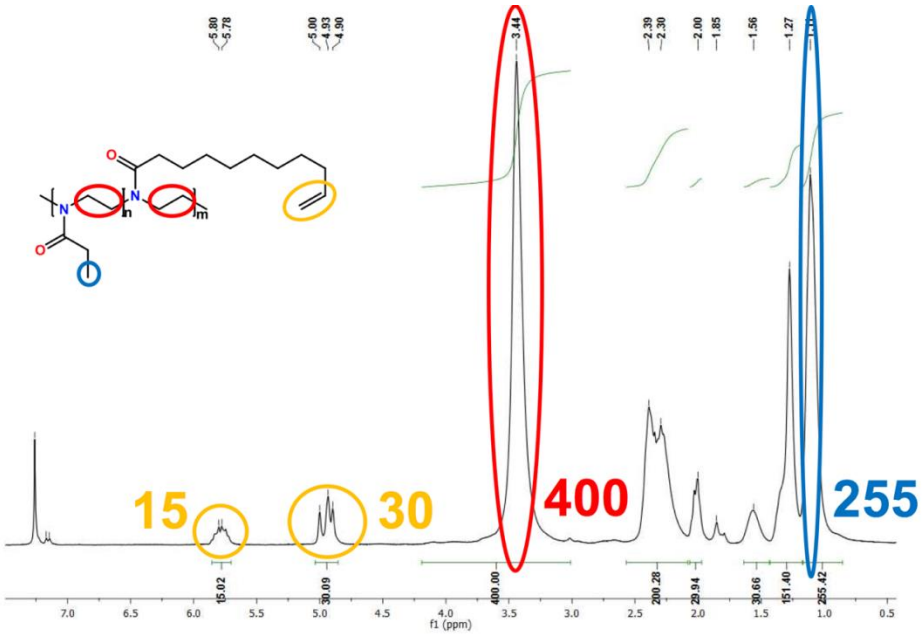

Figure 11: ^{1}H-NMR spectrum of pEtOx$_{85}$-*block*-pDec$^{=}$Ox$_{15}$.

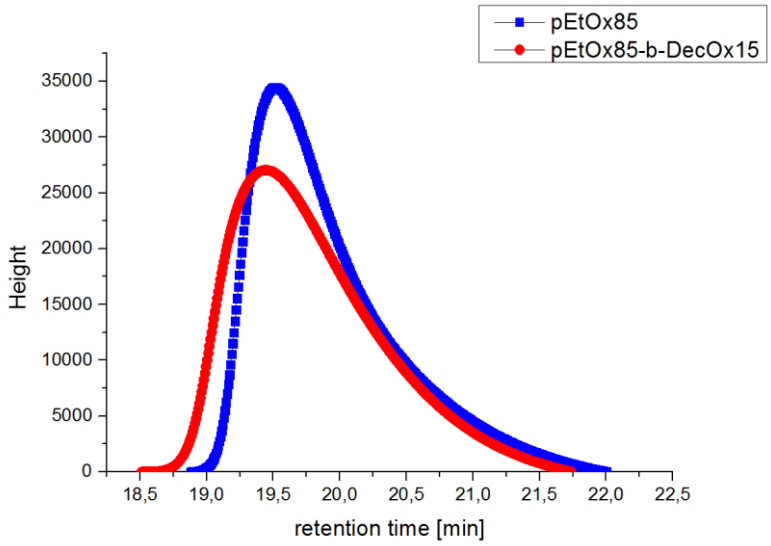

Figure 12: GPC measurement of pEtOx$_{85}$-*block*-pDec$^{=}$Ox$_{15}$.

4.2.4. pEtOx$_{90}$-*block*-p(Dec$^{=}$Ox$_{9}$-*stat*-Pen$^{=}$Ox$_{1}$)

In order to synthesize the mixed block/statistical copoly(2-oxazoline) pEtOx$_{90}$-*block*-p(Dec$^{=}$Ox$_{9}$-*stat*-Pen$^{=}$Ox$_{1}$), Dec$^{=}$Ox and Pen$^{=}$Ox were added simultaneously during the second step of the copolymerization. The verification of the 90:9:1 ratio of the repetition units could be performed by

^{1}H-NMR spectroscopy. Assuming that the polymer back-bone has 400 (= 100·4) hydrogen atoms, the methyl groups of pEtOx show 270 (= 90·3) hydrogen atoms, and the double bonds at the end of pDec$^{=}$Ox have 18 (= 9·2) hydrogen atoms. The alkyne proton of pPen$^{\equiv}$Ox part shows a small peak at 2.16 ppm of 1 hydrogen atom (Figure 13). SEC measurements revealed a PDI value of 1.4 (Figure 14).

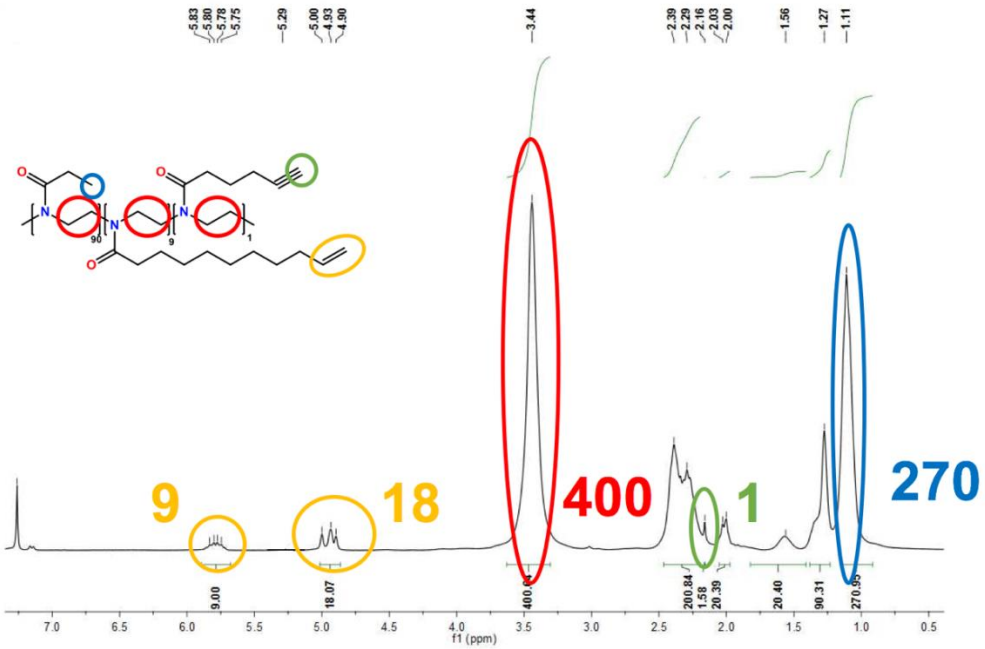

Figure 13: ^{1}H-NMR spectrum of pEtOx$_{90}$-*block*-p(DecOx$_9$-*stat*-PenOx$_1$).

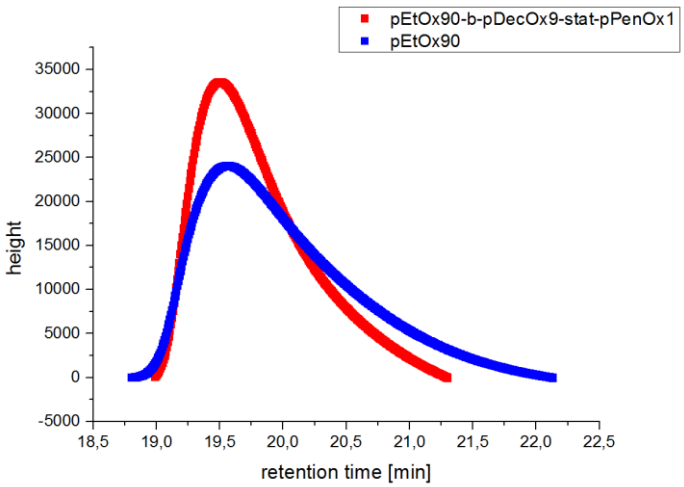

Figure 14: GPC measurement of pEtOx$_{90}$-*block*-p(DecOx$_9$-*stat*-PenOx$_1$).

4.3. Determination of the Critical Micelle Concentration

In order to obtain the critical micelle concentrations CMC, the surface tension of a pending drop of a solution of the respective copoly(2-oxazoline)s was calculated according to Owens-Wendt [109], in dependency on the concentration of the amphiphilic copolymers. Therefore, a calibration row of each copolymer with concentrations from 0.0 to 1.0 $g \cdot L^{-1}$ was prepared, and five measurements per concentration were performed (Figure 15). The average value of surface tension was used to determine the CMC.

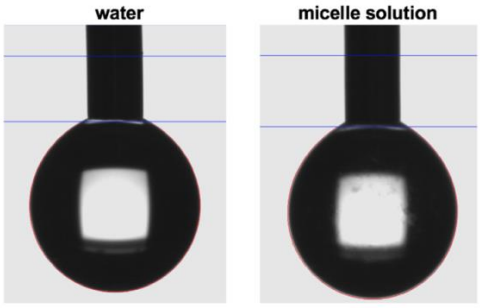

Figure 15: Pending drop of bidistilled water (left) and a micellar solution (right).

For the quantification of the CMC, the surface tension was plotted as function of the concentration of the amphiphilic copolymers (Figure 16).

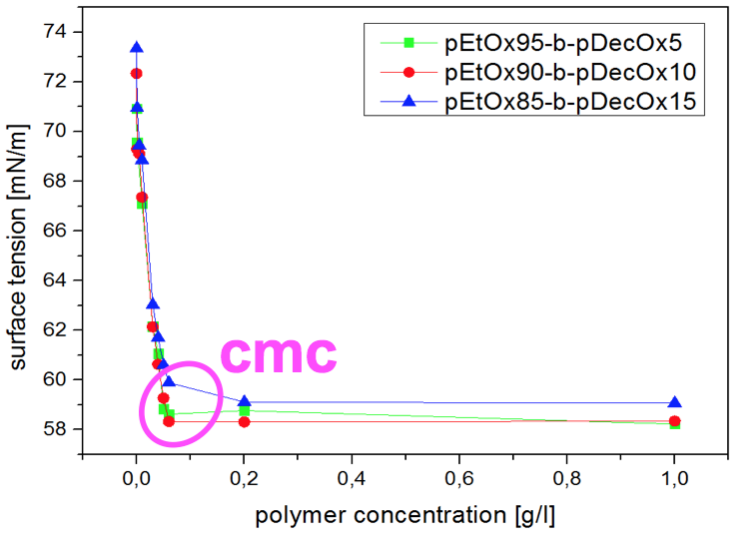

Figure 16: Surface tension of micellar solutions as a function of the polymer concentration.

Initially, the surface tension decreases with increasing copolymer concentration, since the amphiphilic molecules are adsorbed at the water-air interface. After reaching the CMC, the surface tension remains constant despite increasing concentration of the amphiphiles, because the interface is saturated and micellization in the bulk phase occurs [74]. The CMCs were determined for all pEtOx-pDec$^{=}$Ox copolymers (Table 1). As a rule of thumb, the CMC should decrease with increasing hydrophobic block length as the long hydrocarbon chains accelerate aggregation in aqueous media, and the solubility of the amphiphile in water is lowered [110]. Here, it may be assumed that the differences in chain length of the hydrophobic blocks are yet too small to observe this phenomenon.

Table 1: Critical micelle concentrations of the copoly(2-oxazoline)s.

polymer	cmc [g/L]
pEtOx$_{95}$-*block*-pDecOx$_{5}$	0.05
pEtOx$_{90}$-*block*-pDecOx$_{10}$	0.06
pEtOx$_{85}$-*block*-pDecOx$_{15}$	0.06

4.4. Huisgen 1,3 - Dipolar Cycloaddition of Zidovudine to pEtOx$_{90}$-*block*-p(Dec$^{=}$Ox$_{9}$-*stat*-Pen$^{\equiv}$Ox$_{1}$)

The covalent attachment of the pharmaceutically active agent Zidovudine to the alkyne-functionalized copoly(2-oxazoline) occurred via the Huisgen 1,3-dipolar cycloaddition (Scheme 13). pEtOx$_{90}$-*block*-p(Dec$^{=}$Ox$_{9}$-*stat*-Pen$^{\equiv}$Ox$_{1}$) and Zidovudine were dissolved in a DMF:water = 5:1 mixture. After the addition of sodium ascorbate and the catalyst copper(II) sulfate, the reaction mixture was heated to 50 °C and stirred for 1 d. Subsequently, the solvent was removed by reduced pressure, and the raw product was dissolved in DCM, washed with brine (3 times), dried over Na_2SO_4 and filtered. The product could be recovered by repeated solvent

evaporation in satisfying yield and purity and was dried at the vacuum (< 2 mbar) for one day.

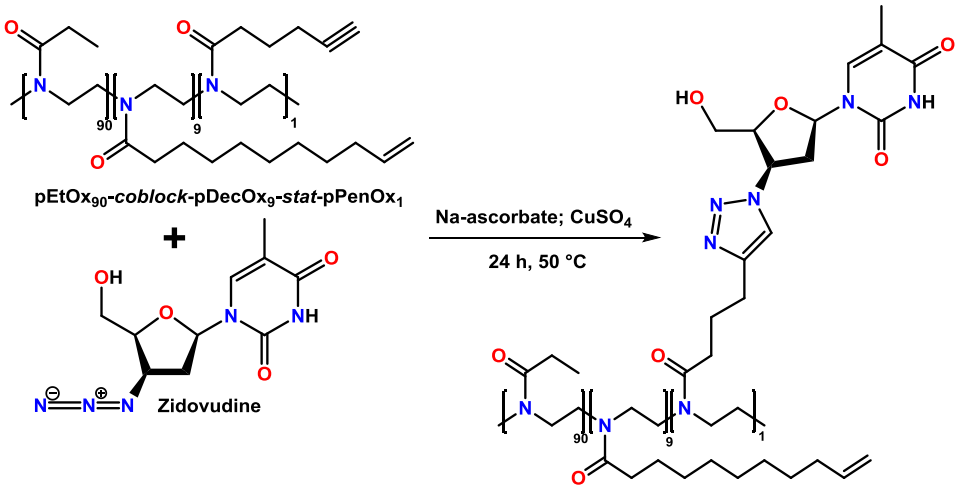

Scheme 13: Schematic representation of the Huisgen 1,3-dipolar cycloaddition.

The ^{1}H-NMR spectrum reveals the absence of the alkyne group of the former pPen$^{=}$Ox block; instead, the signals of the triazole-ring can be observed at approx. 8 ppm. Assuming that the polymer back-bone has 400 (= 100·4) hydrogen atoms, 1 proton of the triazol group can be found, revealing an approx. 50:50 ratio of both isomers (Figure 17).

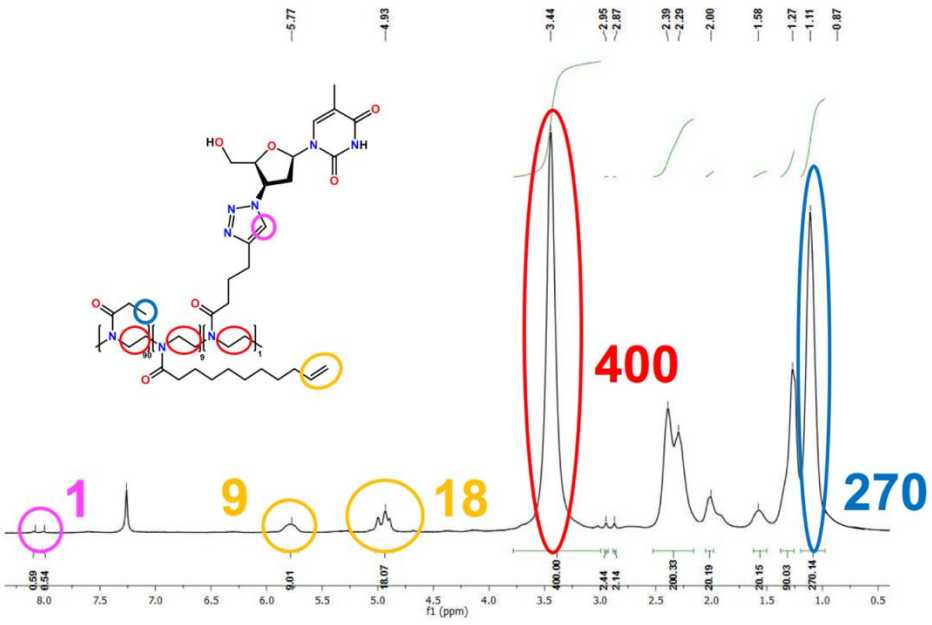

Figure 17: ^{1}H-NMR spectrum of pEtOx$_{90}$-*block*-p(Dec$^{=}$Ox$_{9}$-*stat*-(PenOx-TriAz-Ziduvodine)$_{1}$).

4.5. Results of the Dynamic Light Scattering

4.5.1. Dynamic Light Scattering of Solutions of Non-Crosslinked Amphiphiles

The micelle samples were prepared via the dialysis method. The polymers were dissolved in acetone, and water was added drop-wise under vigorous stirring. Afterwards, the micellar solutions (c = 1 $g \cdot L^{-1}$) were dialyzed against water for 3 d. Dynamic light scattering was measured by Franz Pirolt with a diode laser at 90° and a resolution of 43 nm (q_{min} = 0.073) for 30 min (30 frames, 60 s exposure time). 10 measurements (30 s) were conducted per sample, and the median was calculated. All samples showed a depolarized light signal, evident of anisotropic structures. Such structures can be formed by block copolymers if the hydrophobic block is significantly shorter than the hydrophilic one [78] or due to hydration and swelling of the corona that imparts curvature to the amphiphile to form worm-like micelles [76]. The hydrodynamic radii R_H were calculated using the second cumulant method on the averaged correlation function. The hydrodynamic radii of the non-crosslinked samples increased with increasing hydrophobic block length (Table 2). This observation was referred to the fact that the longer side-chains of the hydrophobic block interact and need more space [110]. In general, an increase of the depolarized signal with increasing hydrodynamic radius can be observed. It can be assumed that worm-like micelles are formed.

Table 2: Hydrodynamic radii and depolarized light signal of non-crosslinked samples in water.

Sample	R_H [nm]*	Depolarized DLS**
$pEtOx_{95}$-b-$pDecOx_5$	82.40 ± 0.13	200-300 Hz
$pEtOx_{90}$-b-$pDecOx_{10}$	90.52 ± 0.27	3.3-4 kHz
$pEtOx_{85}$-b-$pDecOx_{15}$	106.03 ± 0.25	9.5 kHz

*calculated by 2nd cumulant fit, using an averaged correlation function;
** 0.12 W Power.

4.5.2. Dynamic Light Scattering of Solutions of Crosslinked Amphiphiles

The crosslinked micelle samples were also prepared via the dialysis method. In addition to the polymer, the crosslinker glycol dimercaptoacetate GDMA (Figure 18) and the photoinitiator Lucirin TPO-L were dissolved in acetone, notably under the exclusion of light irradiation. Afterwards, water was added drop-wise under vigorous stirring, and the micellar solutions were dialyzed against water for 3 d without light irradiation. The 1 $g \cdot L^{-1}$ solutions were stirred and illuminated (1 h, 5000 $mW \cdot cm^{-2}$, 10 cm) to start the crosslinking between the alkene functions of pDec$^{=}$Ox and the thiols of GDMA (chapter 3.4.1.).

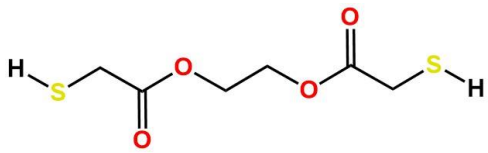

Glycol dimercaptoacetate (GDMA)

Figure 18: Used bi-functional thiol (GDMA) for the crosslinking of the micelles

Dynamic light scattering was measured under the same conditions like for the non-crosslinked amphiphiles. The hydrodynamic radii of the crosslinked samples increased with decreasing hydrophobic block lengths, and the depolarized light signal increased (again) with increasing hydrodynamic radius (Table 3). Since depolarization can be detected, worm-like micelles were assumed to be formed.

Table 3: Hydrodynamic radii and depolarized light signal of crosslinked samples in water.

Sample	RH [nm] *	Depolarized DLS [kHz] **
pEtOx$_{95}$-*b*-pDec$^{=}$Ox$_5$	101.86 ± 0.22	7
pEtOx$_{90}$-*b*-pDec$^{=}$Ox$_{10}$	95.86 ± 0.17	6
pEtOx$_{85}$-*b*-pDec$^{=}$Ox$_{15}$	72.53 ± 0.13	5

(*calculated by 2nd cumulant fit, using an averaged correlation function;
** 0.12 W Power)

4.5.3. Comparison of the Dynamic Light Scattering of Solutions of Non-Crosslinked and Crosslinked Amphiphiles

This reverse trend of the R_H size of crosslinked micelles compared to non-crosslinked micelles in aqueous solution (Figure 19) is assumed to originate from the fact that the crosslinking (of the cores) results in a more dense packing of the micelles and, consequently, that the association tendency between the hydrophobic segments increases with higher hydrophobic content [111;112], resulting in a decrease of the hydrodynamic radii. This effect is most pronounced in case of the pEtOx$_{85}$-*block*-pDec$^{=}$Ox$_{15}$ copolymer, which contains the longest hydrophobic block and, hence, achieves the highest crosslinking degree of the three copolymers of this series. The R_H of crosslinked pEtOx$_{85}$-*block*-pDec$^{=}$Ox$_{15}$ is the smallest one, whereas the hydrodynamic radius of crosslinked pEtOx$_{95}$-*block*-pDec$^{=}$Ox$_{5}$ is the highest and considerably higher than its non-crosslinked analogue (Figure 19). It can be assumed that the association tendency between only 5 hydrophobic repetition units is too weak for closer packing in the course of crosslinking [112].

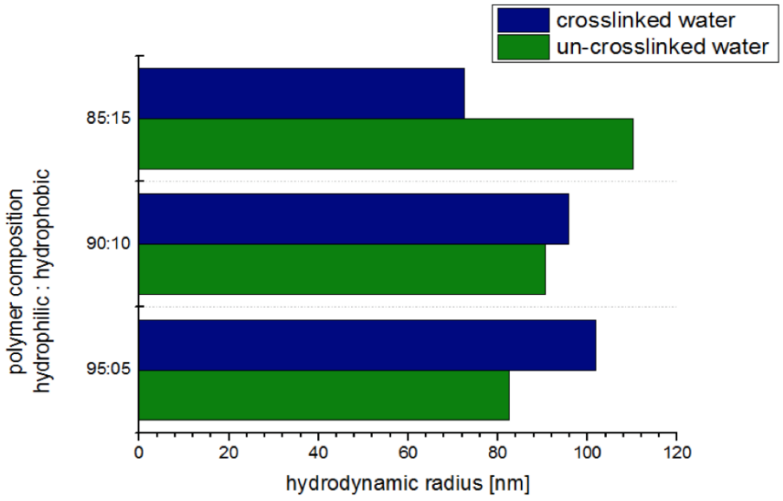

Figure 19: Hydrodynamic radii of crosslinked micelles compared to non-crosslinked ones.

4.5.4. Dynamic Light Scattering of Solutions of Non-Crosslinked and Crosslinked Amphiphiles after Oil Uptake

Aiming to verify the crosslinking of the micelles by the thiol-ene reaction with GDMA, crosslinked as well as non-crosslinked micellar solutions were vigorously stirred in oil (water/oil v:v = 1:1) for 7 d. Theoretically, the crosslinked samples should have a lower oil uptake than the non-crosslinked ones as a consequence of the higher rigidity due to the covalent bonds formed during the crosslinking reaction.

After 7 d, the changes of the hydrodynamic radii were determined via DLS measurements. The R_H of crosslinked as well as non-crosslinked micelles increased (Table 4), which is caused by the oil uptake of the micelles' core.

Table 4: Hydrodynamic radii of crosslinked and non-crosslinked micelles in an oil/water (1:1) emulsion.

Sample		RH [nm] *	Depolarized DLS [kHz] **
CL* **	**pEtOx$_{95}$-b-pDec$^{=}$Ox$_5$**	486.61 ± 3.57	13
non-CL * **	**pEtOx$_{95}$-b-pDec$^{=}$Ox$_5$**	815.47 ± 4.52	80
CL* **	**pEtOx$_{90}$-b-pDec$^{=}$Ox$_{10}$**	185.94 ± 1.69	4.3
non-CL * **	**pEtOx$_{90}$-b-pDec$^{=}$Ox$_{10}$**	726.41 ± 2.11	55
CL* **	**pEtOx$_{85}$-b-pDec$^{=}$Ox$_{15}$**	114.53 ± 0.27	4
non-CL * **	**pEtOx$_{85}$-b-pDec$^{=}$Ox$_{15}$**	110.21 ± 0.25	4.5

*calculated by 2nd cumulant fit, using an averaged correlation function;
** 0.12 W Power;
*** CL: crosslinked; non-CL: non-crosslinked.

The hydrodynamic radii of the non-crosslinked micelles are significantly higher in case of the polymers pEtOx$_{95}$-*block*-pDec$^{=}$Ox$_5$ and pEtOx$_{90}$-*block*-pDec$^{=}$Ox$_{10}$ (Figure 20), indicative of a successful crosslinking. The hydrodynamic radii of pEtOx$_{85}$-*block*-pDec$^{=}$Ox$_{15}$, however, are of the same range, maybe due to the generally higher association tendency of the hydrophobic chains in this copolymer [112].

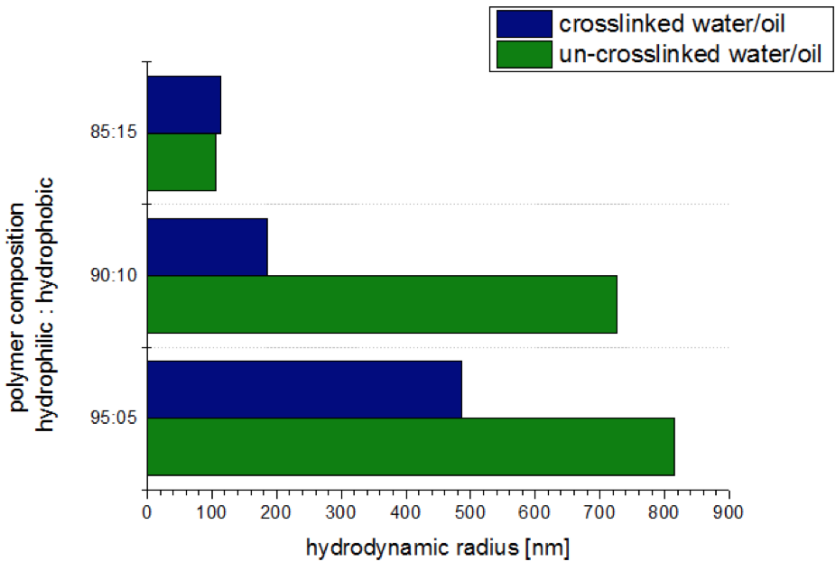

Figure 20: Hydrodynamic radii of crosslinked micelles compared to non-crosslinked micelles in an oil/water (1:1) emulsion.

4.5.5. Dynamic Light Scattering of the Amphiphile Containing the API Zidovudine

Micellization of the copoly(2-oxazoline) with the incorporated active agent Zidovudine, and its crosslinking were performed like described hereinabove according the dialysis method. The hydrodynamic radii were determined by DLS measurements, too. The same phenomena as before could be observed: The crosslinked micelles (130.37 ± 0.28 nm) are considerably smaller than the non-crosslinked analogues (161.64 ± 0.41 nm) (Figure 21), whereat both micelle types are significantly larger than those of the similar copolymer $pEtOx_{90}$-*block*-$pDec^{=}Ox_{10}$ (90-95 nm). The increased hydrodynamic radii could be a result of the incorporation of the polar active agent Zidovudine (Figure 22). Such a hindrance parameter influences the degree of flexibility and increases the rotation barrier. The thread end distances are also increasing due to the interactions of the polar molecules with the hydrophilic block [112].

A detailed investigation reveals that Pen$^{=}$Ox is hydrophilic, and that Zidovudine consists of amino- and hydroxyl-functionalities, which can form hydrogen bridges. Due to their incorporation in the *core* of the micelle, the interactions of the polar groups might be reasonable for the elongation of the worm-like structure, which would increase the hydrodynamic radii. The R_H of the crosslinked Zidovudine-containing block copolymer is smaller than that of the non-crosslinked one, like it is the case in the pEtOx$_{85}$-*block*-pDec$^{=}$Ox$_{15}$. The crosslinking within the chains leads to the closer packing of the micelles, and hence, the association tendency between the hydrophobic segments increases [111;112], and the hydrodynamic radii decrease. Moreover, also in case of these micelles, a depolarized signal in dependency on the size could be detected; therefore it can be assumed that worm-like micelles were formed.

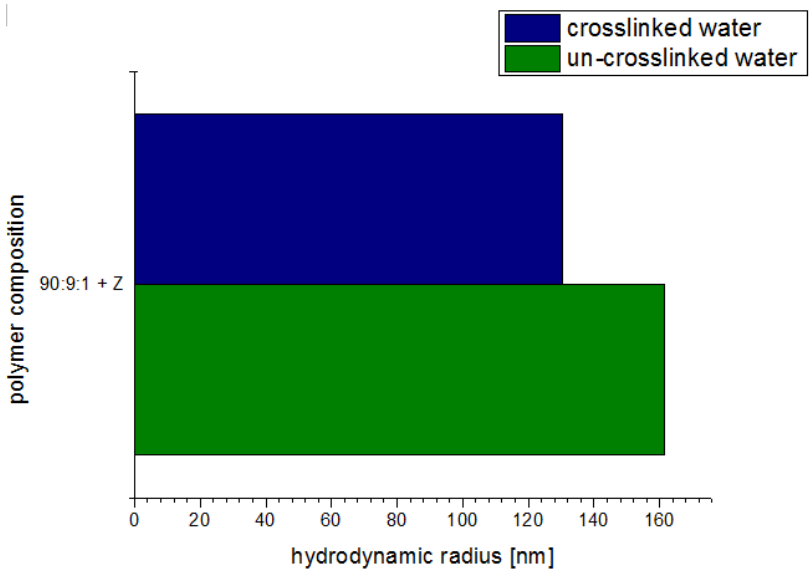

Figure 21: Hydrodynamic radii of crosslinked and non-crosslinked micelles of the triblock copolymer with incorporated Z = Zidovudine.

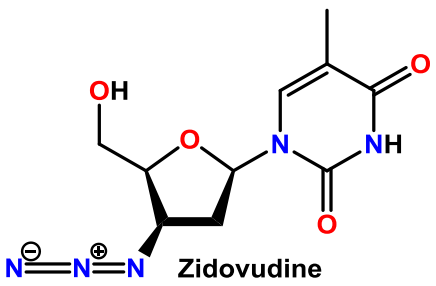

Figure 22: Structure of Zidovudine.

5. Conclusions and Outlook

The scope of this master thesis was a first investigation of the potential application of non-crosslinked as well as crosslinked poly(2-oxazoline)-based micelles as new drug delivery systems: This research was particularly motivated by the high biocompatibility of this polymer class.

Three 2-oxazoline monomers were used for the synthesis of amphiphilic block copoly(2-oxazoline)s: The hydrophilic monomers 2-ethyl-2-oxazoline EtOx and 2-pent-4'ynyl-2-oxazoline Pen$^{=}$Ox are commercially available, whereas the hydrophobic monomer 2-dec-9'-enyl-2-oxazoline Dec$^{=}$Ox was synthesized according to the Henkel Patent [15], which has the big advantages that no solvent is needed and renewable resources can be used as reactants. The polymerizations were performed in a microwave reactor, which results in a higher polymerization rate, no limitation of the temperature by the boiling point of the solvent, and autoclave conditions. Since the polymerization of poly(2-oxazoline)s proceeds via the pseudo-living cationic ring opening mechanism, the synthesis of amphiphilic block copolymers was carried out by consecutively incorporating the monomers under inert conditions. Three diblock copolymers with varying hydrophilic/hydrophobic block length, namely pEtOx$_{95}$-*block*-pDec$^{=}$Ox$_5$, pEtOx$_{90}$-*block*-pDec$^{=}$Ox$_{10}$, and pEtOx$_{85}$-*block*-pDec$^{=}$Ox$_{15}$, as well as the mixed block/statistical copolymer pEtOx$_{90}$-*block*-p(Dec$^{=}$Ox$_9$-*stat*-Pen$^{=}$Ox$_1$) could be successfully synthesized. These amphiphilic polymers form micellar structures with a hydrophobic core and a hydrophilic corona in aqueous solutions via self-assembly (Figure 23).

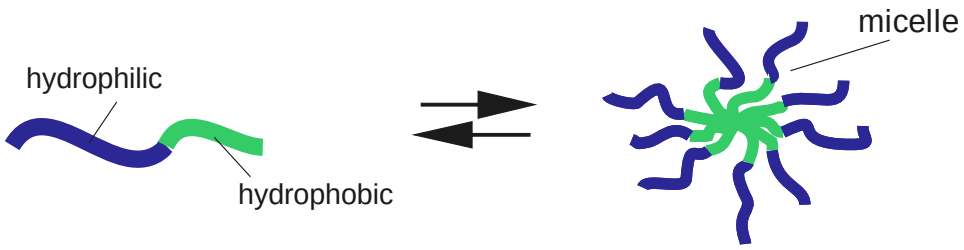

Figure 23: Self-assembly of amphiphilic polymers.

To determine their critical micelle concentration CMC, which is an important factor according the stability of a micellar system, the surface tension of a pending drop was determined in dependency on the concentration of the amphiphilic copolymers. A typical progression of the surface tension could be observed (Figure 24). The surface tension decreased with increasing amphiphilic polymeric concentration until the interface water-air was saturated with amphiphiles, and the formation of micelles started in the bulk phase. After the micellization had started, the surface tension stayed constant, even if the concentration of the polymer increased. The observed critical micelle concentrations for the three diblock copolymers ranged from 0.05 to 0.06 $g \cdot L^{-1}$.

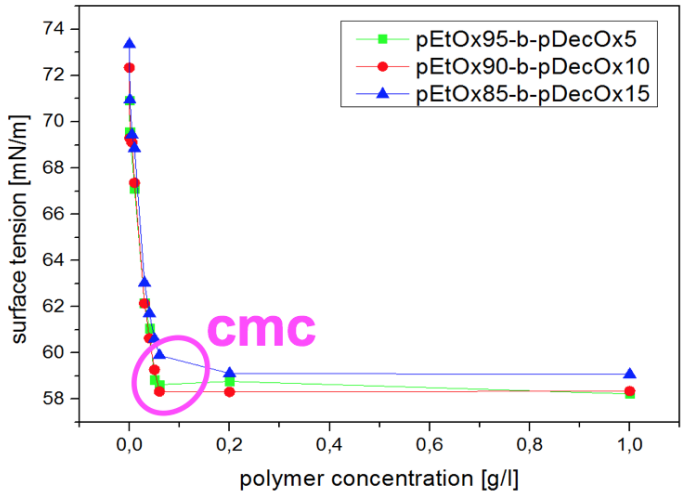

Figure 24: Determination of the CMC by measuring the surface tension of a pending drop in dependency of the concentration of amphiphilic co polymers.

Benefiting from the different functionalities in the side-chains of the individual blocks, the polymers/micelles could be modified by two different orthogonal synthesis strategies. Via the UV-light induced thiol-ene click reaction, the alkene functionality in the side-chain of the pDec$^{=}$Ox block could be reacted with (multifunctional) thiols to yielding crosslinked systems in aqueous media, which increases the stability of a micelle, even in very diluted systems. As crosslinker, glycol dimercaptoacetate GDMA with hydrolysable ester bonds (Figure 25) was used.

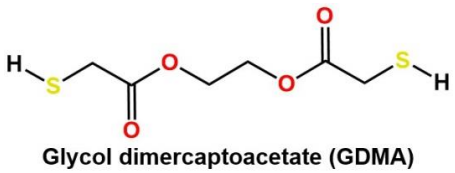

Figure 25: Structure of GDMA, used for the crosslinking by the thiol-ene click reaction.

The second polymeranalogous reaction was the Huisgen 1,3-dipolar cycloaddition aiming to incorporate the pharmaceutically active agent Zidovudine within the polymeric matrix (pPen$^{=}$Ox repetition units). The copper(II)-catalyzed reaction of the azide function of Zidovudine with the alkyne functionality in the pPenOx block of the copolymer yielded the corresponding triazoles.

In order to determine the hydrodynamic radii of the micelles formed by different amphiphilic block copolymers (crosslinked/non-crosslinked diblock copolymers and crosslinked/non-crosslinked mixed block/statistical copolymers with covalently attached Zidovudine), dynamic light scattering DLS measurements were performed. The radii of the non-crosslinked micelles of the diblock copolymers increased with increasing hydrophobicity of the copolymer, whereas the crosslinked micelles of these polymers behaved opoosite (Figure 26). This reverse trend in R_H - size of crosslinked micelles compared to non-crosslinked micelles in aqueous solution can be explained by the assumption that the crosslinked cores can be packed in more dense fashion, which increases the association tendency between the hydrophobic segments. This effect is more pronounced if the hydrophobic blocks grow (relatively) larger. The hydrodynamic radii of the micelles of the amphiphilic mixed block/statistical copolymer are generally larger than those of the corresponding diblock copolymer (pEtOx$_{90}$-*block*-pDec$^{=}$Ox$_{10}$). The larger radii could be a result of the incorporation of the polar active agent Zidovudine and the correspondingly increased polar interactions in the hydrophobic core.

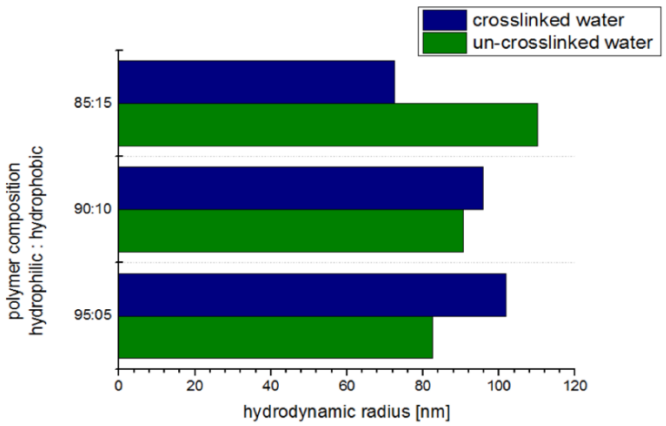

Figure 26: Comparison of the hydrodynamic radii of the crosslinked and non-crosslinked micelles of the diblock copolymers.

The crosslinking of the micelles was tested by stirring the aqueous micellar solutions with oil (1:1 mixture) for one week. In general, the R_H of the non-crosslinked micelles increased drastically in comparison to the crosslinked ones, which was referred to the lowered structural flexibility after crosslinking. Only the crosslinked and un-crosslinked micelles of $pEtOx_{85}$-*block*-$pDecOx_{15}$ were in the same dimension. In all cases, a depolarized signal could be detected, therefore it can be assumed that worm-like micelles were formed.

In further works, transmission electron microscopy images and atomic force microscopy images of the obtained micelles could be measured as an alternative technique for the structure determination. Moreover, compound release studies could be started by hydrolysis or other stimuli such as temperature, pH, etc. Since these drug delivery systems should be able to be introduced into an organism, also cytotoxicity studies and biodegradation studies should be done. The block length of the polymers could be varied to form spherical micelles too; other monomers like 2-but-3'-enyl-2-oxazoline $Bu^{=}Ox$, MeOx or NonOx could be used to synthesize reverse micelles or corona-crosslinked micelles.

6. Abstract

The aim of this work was the development of crosslinked poly(2-oxazoline)-based micelles as new drug delivery systems. Due to the high biocompatibility of this polymer class, they are a potential alternative to the already widely studied poly(ethylene glycol) for medic(in)al applications. The large variety of 2-oxazoline monomers enables the synthesis of polymers with specific properties. For the formation of micelles, amphiphilic block copolymers need to be synthesized via the pseudo-living cationic ring-opening polymerization of 2-oxazolines. In this thesis, 2-ethyl-2-oxazoline EtOx and 2-pent-4'-ynyl-2-oxazoline PenOx were selected as hydrophilic monomers, and 2-dec-9'-enyl-2-oxazoline DecOx was chosen as hydrophobic one. These 2-oxazoline monomers were copolymerized in different contents. Via self-assembly, the diblock copolymers ($pEtOx_{95}$-*block*-$pDecOx_5$, $pEtOx_{90}$-*block*-$pDecOx_{10}$, $pEtOx_{85}$-*block*-$pDecOx_{15}$) formed worm-like micelles with hydrodynamic radii from 82 to 106 nm in aqueous media with a critical micelle concentration CMC of 0.05-0.06 g/L. Due to the alkene function in the side-chain of the pDecOx block, the micelles could be crosslinked by the UV-light induced thiol-ene click reaction. While the radii of the non-crosslinked micelles increased with the hydrophobicity of the polymer, the crosslinked micelles became smaller with increasing hydrophobicity (radii from 70 to 100 nm), due to closer-packing by crosslinking and the stronger association tendency of the hydrophobic block. Moreover, an amphiphilic block copolymer of the composition $pEtOx_{90}$-*block*-p($DecOx_9$-*stat*-$pPenOx_1$) was synthesized to covalently attach the pharmaceutically active agent Zidovudine via the Huisgen 1,3-dipolar cycloaddition. The micelles of this polymer were generally larger than those of the similar diblock copolymer $pEtOx_{90}$-*block*-$pDecOx_{10}$, which was assumed to result from the introduction of a polar molecule into the hydrophobic core.

7. Kurzfassung

Ziel dieser Arbeit war die Herstellung vernetzter Mizellen basierend auf der Polymerklasse der Poly(2-oxazolin)e als neue Wirkstofftransport-systeme. Aufgrund der hohen Biokompatibilität dieser Polymere handelt es sich hierbei um eine vielversprechende Alternative für bisher erforschte Systeme auf Basis von Poly(ethylenglykol). Durch die große Vielfalt an Monomeren, können maßgeschneiderte Poly(2-oxazolin)e mit speziellen Eigenschaften synthetisiert werden. Da die Polymerisation über einen pseudo-lebenden kationischen ringöffnenden Mechanismus erfolgt, ist die Herstellung amphiphiler Block-Copolymere möglich. Als hydrophile Monomere wurden 2-Ethyl-2-oxazolin EtOx und 2-Pent-4'-inyl-2-oxazolin PenOx ausgewählt; 2-Dec-9'-enyl-2-oxazoline DecOx stellte das hydrophobe Monomer. Aus diesen Monomeren wurden drei verschiedene Diblock-Copolymere synthetisiert, $pEtOx_{95}$-*block*-$pDecOx_5$, $pEtOx_{90}$-*block*-$pDecOx_{10}$ und $pEtOx_{85}$-*block*-$pDecOx_{15}$. Durch *self-assembly* ordnen sich die amphiphilen Polymere in wässriger Lösung zu wurmartigen Mizellen an, deren kritische Mizellbildungskonzentration CMC im Bereich von 0.05 bis 0.06 g/L liegt. Aufgrund der Doppelbindungen im pDecOx-Block können die Mizellen mittels der UV-induzierten Thiol-en Click-Reaktion vernetzt werden und bilden danach ein stabiles Transportmedium aus. Während der hydrodynamische Radius der unvernetzten Mizellen mit dem hydrophoben Anteil steigt, sinkt dieser in vernetzten wurmartigen Mizellen mit stärkerer Hydrophobie. Dies ist vermutlich darin auf das Vernetzen des hydrophoben Blocks und die damit einhergehende erhöhte Packungsdichte Assoziationstendenz der hydrophoben Segmente zurückzuführen. Außerdem wurde ein gemischtes statistisches/Block-Copolymer synthetisiert: $pEtOx_{90}$-*block*-p($DecOx_9$-*stat*-$PenOx_1$), an welches mittels der Huisgen 1,3-dipolaren Zykloaddition Zidovudin als Wirkstoff gebunden wurde. Die Mizellen dieses Polymers waren im Vergleich mit den typähnlichen Mizellen des Diblock-Copolymers $pEtOx_{90}$-*block*-$pDecOx_{10}$ deutlich größer, jedoch konnte auch hier wieder eine Verringerung des hydrodynamischen Radius bei Vernetzung erzielt werden.

8. Experimental

8.1. Used Chemicals

Table 5: List of used chemicals.

Substance	Resource	Purity	Note
10-undecenacid	Sigma-Aldrich, Austria	97%	
2-aminoethanol	Sigma-Aldrich, Austria	98%	
2-ethyl-2-oxazoline	ABCR	99%	
acetonitrile	Carl Roth	99,50%	
chloroform	AnalaR Normapur		
decanoic acid	SFC		
dichloromethane	Fischer Chemicals		
glycol dimercaptoacetate	Bruno Bock, Germany		
methanol	Chem Lab	HPLC	
methyl tosylate	Sigma-Aldrich, Austria	98%	distilled
sodium sulphate	Sigma-Aldrich, Austria	99,90%	
titanium(IV)butoxide	Sigma-Aldrich, Austria	99%	
zidovudine	Sigma-Aldrich, Austria		
2-(pent-4-ynyl)-2-oxazoline	Sigma-Aldrich, Austria	96%	distilled
dimethylformamide	Carl Roth	99,8%	
copper(II)sulfate	Sigma-Aldrich, Austria	99%	
sodium-L-ascorbate	Fluka BioChem	99%	

8.2. Used Methods for Analysis and Synthesis

NMR Analysis: For the measurement of the NMR-spectra, a Bruker Advance III 300 MHz spectrometer with an auto sampler was used. The samples were dissolved in deuterated chloroform, the residual signal of which was used as a reference signal at 7.26 ppm in the ^{1}H-NMR spectra and at 77 ppm in the ^{13}C-NMR spectra.

Infrared Spectroscopy: The infrared spectra were recorded with a Bruker Alpha Fourier-Transform Infrared Spectrometer with ATR support. A wavelength area from 375-4000 cm^{-1} with 32 scans per measurement was used . The background was measured before each measurement.

Microwave-assisted synthesis: The synthesis of the polymers was performed in the Biotage Initiator 8 microwave reactor with auto sampler. The reaction parameters depend on the synthesis and are described in the synthesis part. The vials with a maximum volume of 5 mL were dried at 80 °C prior to use. The educts were weighted in gravimetrically under inert conditions. The reaction mixture was mixed via a stirring bar at 600 rpm. The temperature was controlled with an internal infrared sensor.

UV-induced crosslinking: The experiments were performed with an EFOS Novacure UV Hg/Xe Lamp of EXFO. The samples were stirred under UV-light at 5000 $mW \cdot cm^{-2}$ for 1 h under vigorous stirring. The distance between the reaction medium surface and lamp was 10 cm.

Gel permeation chromatography: A Merck Hitachi L-6000A pump, a Polymer Standards Service column (8\300 mm STV linear XL 5 µm-grade size) and a differential refractometer Waters 410 detector were used for the measurements. For the calibration, a polystyrene standard of Polymer

Standard Service was applied; a mixture of $CHCl_3$/Et_3N/$^{iso}PrOH$ (94/4/2) was used as eluent.

Thermal Analysis: The thermograms of the polymers were recorded with a Perkin Elmer DSC 4000 with auto sampler. The measurements were performed under N_2 atmosphere in a temperature range from –50 to 100 °C with a heating rate of 10 $K \cdot min^{-1}$.

Critical Micelle Concentration: To determine the surface tension of a pending drop, a KRÜSS DSA100 with Drop Shape Analysis program was used. For calculating the critical micelle concentration, the surface tension of each polymer solution (calibration from 0.0 to 1 $g \cdot L^{-1}$) was measured 5 times; the mean value was plotted against the concentration of the polymer in water.

Dynamic Light Scattering: The samples were measured with a diode laser (Coherent Verdi V5, λ = 532 nm) at 90°. The scattered light was guided through a single-mode fiber to an ALV/SO-SIPD/DUAL photomultiplier with pseudo-cross correlation and correlated by an ALV 7004 Digital Multiple Tau Real Time Correlator (ALV, Langen, Germany). 10 measurements (30 s) were conducted per sample and averaged. The hydrodynamic radius R_H was calculated from the second cumulant method on the averaged correlation function.

8.3. Synthesis of 2-Dec-9'-enyl-2-oxazoline Dec$^{=}$Ox

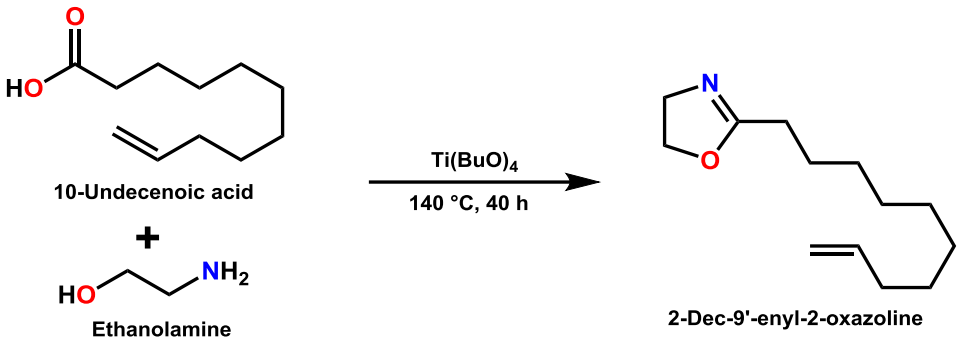

Scheme 14: Synthesis of 2-Dec-9'-enyl-2-oxazoline.

The synthesis was done according to the Henkel patent [15]. 10-Undecenoic acid (91.3 g; 100 mL; 0.5 mol) and ethanolamine (45.0 g; 44.8 mL; 0.73 mol) were weighed into a 500 mL flask. Titanium(IV)-^{n}butoxide (0.91 g; 2.7 mmol) was added, and the reaction mixture was heated to 140 °C. The mixture was stirred for 24 h under reflux. For complete conversion of the educts, Titanium(IV)-^{n}butoxide (1.0 g; 2.9 mmol) were added again after 15 and 20 h. For removal of the water, the cooler was removed and the reaction mixture was stirred at 140 °C for 16 h. The recovery and purification of the product was achieved by distillation under reduced pressure at 180 °C and < 2 mbar.

^{1}H-NMR (300 MHz, $CDCl_3$): δ (ppm) = 1.20-1.40 (10 H, m, -CH_2-), 1.52-1.68 (2 H, m, -CH_2-C*H*$_2$-CH_2-C=), 1.96-2.02 (2 H, m, -CH_2-C*H*$_2$-CH=), 2.24 (2 H, t, -C=C*H*$_2$-CH_2-), 3.79 (2 H, t, -O-C*H*$_2$-CH_2-N=), 4.19 (2 H, t, -O-CH_2-C*H*$_2$-N=), 4.86-5.00 (2 H, m, -CH=C*H*$_2$), 5,90-5.70 (1 H, m, -C*H*=CH_2).

^{13}C NMR (75 MHz, $CDCl_3$): δ (ppm) = 20.4, 29.3, 29.6, 32.4, 33.9, 53.8, 68.1, 115.7, 139.1, 173.7.

IR (ATR): ν (cm^{-1}) = 2921, 2852, 1641, 1463, 1430, 1182, 1160, 909, 772, 721.

8.4. Synthesis of the Diblock Copoly(2-oxazoline)s

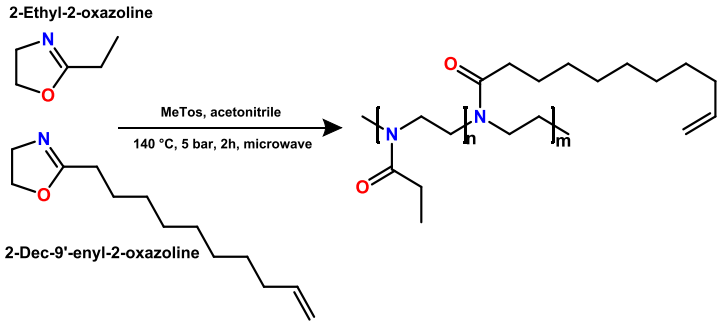

Scheme 15: Synthesis of $pEtOx_n$-*block*-$pDec^{=}Ox_m$.

8.4.1. Synthesis of $pEtOx_{95}$-*block*-$pDec^{=}Ox_5$

A 5 mL Biotage reaction vial was dried in an oven at 80 °C for 30 min. Afterwards, the dried vessel was flushed with argon; 1.80 g (0.02 mol) EtOx, dissolved in 2 mL of acetonitrile, and 35.59 mg (1.9 mmol) MeOTs were weighed in under inert conditions. The vial was crimped and placed in the Biotage microwave reactor. After 5 s of pre-stirring, the reaction mixture was heated to 140 °C for 1 h. The conversion was controlled via NMR-spectroscopy. Subsequently, under inert conditions, 0.203 g (1 mmol) $Dec^{=}Ox$, dissolved in 0.5 mL of acetonitrile, were added to the reaction vial. The mixture was pre-stirred for 5 s in the microwave reactor and then heated to 140 °C for 1 h. The solvent was evaporated under reduced pressure (< 2 mbar), and the polymer was obtained as a white solid.

^{1}H NMR (300 MHz, $CDCl_3$): δ = 5.79 (1H), 5.02-4.88 (2H), 3.44 (80H), 2.34 (38H), 2.00 (4H), 1.56 (2H), 1.27 (10H), 1.11 (57H).

^{13}C NMR (76 MHz, $CDCl_3$) δ = 174.6, 173.9, 45.3, 33.8, 29.4, 29.1, 28.9, 26.0, 9.5.

IR: (ATR) ν (cm^{-1}) = 2922, 2852, 1641, 1463, 1430, 1182, 1161, 909, 772, 721.

GPC: M_w = 6106 g·mol^{-1}; M_n = 4296 g·mol^{-1}; PDI = 1.4

8.4.2. Synthesis of $pEtOx_{90}$-*block*-$pDecOx_{10}$

A 5 mL Biotage reaction vial was dried in an oven at 80 °C for 30 min. Afterwards, the dried vessel was flushed with argon and 1.620 g (0.02 mol) EtOx, dissolved in 2 mL of acetonitrile, and 38.00 mg (2 mmol) MeOTs were weighed in under inert conditions. The vial was crimped and placed in the Biotage microwave reactor. After 5 s of pre-stirring, the reaction mixture was heated to 140 °C for 1 h. Subsequently, under inert conditions, 0.385 g (1.8 mmol) $Dec^{=}Ox$, dissolved in 0.5 mL of acetonitrile, were added to the reaction vial. The mixture was pre-stirred for 5 s in the microwave reactor and then it was heated to 140 °C for 1 h. The solvent was evaporated under reduced pressure (< 2 mbar), and the polymer was obtained as white solid.

^{1}H NMR (300 MHz, $CDCl_3$): δ = 5.79 (1H), 5.03-4.86 (2H), 3.44 (40H), 2.56-2.03 (20H), 2.02 (2H), 1.57 (2H), 1.28 (9H), 1.11 (27H).

^{13}C NMR (76 MHz, $CDCl_3$): δ = 174.6, 173.9, 114.1, 45.8, 43.6, 33.8, 29.4, 26.0, 9.5.

IR: (ATR) ν (cm^{-1}) = 2921, 2851, 1641, 1463, 1430, 1183, 1161, 909, 772, 721.

GPC: M_w = 5875 g·mol^{-1}; M_n = 4021 g·mol^{-1}; PDI = 1.5

8.4.3. Synthesis of $pEtOx_{85}$-*block*-$pDecOx_{15}$

A 5 mL Biotage reaction vial was dried in an oven at 80 °C for 30 min. Afterwards, the dried vessel was flushed with argon and 1.446 g (0.02 mol) EtOx, dissolved in 2 mL of acetonitrile, and 32.20 mg (1.7 mmol) MeOTs were weighed in under inert conditions. The vial was crimped and placed in the Biotage microwave reactor. After 5 s of pre-stirring, the reaction mixture was heated to 140 °C for 1 h. Subsequently, under inert conditions, 0.546 g (2.6 mmol) $Dec^{=}Ox$, dissolved in 1 mL of acetonitrile,

were added to the reaction vial. The mixture was pre-stirred for 5 s in the microwave reactor and then it was heated to 140 °C for 1 h. The solvent was evaporated under reduced pressure (< 2 mbar), and the polymer was obtained as white solid.

^{1}H NMR (300 MHz, $CDCl_3$): δ = 5.79 (3H), 5.03-4.85 (6H), 3.44 (80H), 2.34 (40H), 2.00 (6H), 1.56 (6H), 1.27 (30H), 1.11 (51H).

^{13}C NMR (76 MHz, $CDCl_3$): δ = 174.6, 174.4, 174.1, 152.8, 114.1, 45.4, 33.8, 29.6, 29.0, 26.0, 25.3, 9.5.

IR (ATR): ν (cm^{-1}) = 2922, 2853, 1641, 1463, 1431, 1182, 1161, 909, 772, 721.

GPC: M_w = 6992 g·mol^{-1}; M_n = 5139 g·mol^{-1}; PDI = 1.4

8.4.4. Synthesis of pEtOx$_{90}$-*block*-p(DecOx$_9$-*stat*-PenOx$_1$)

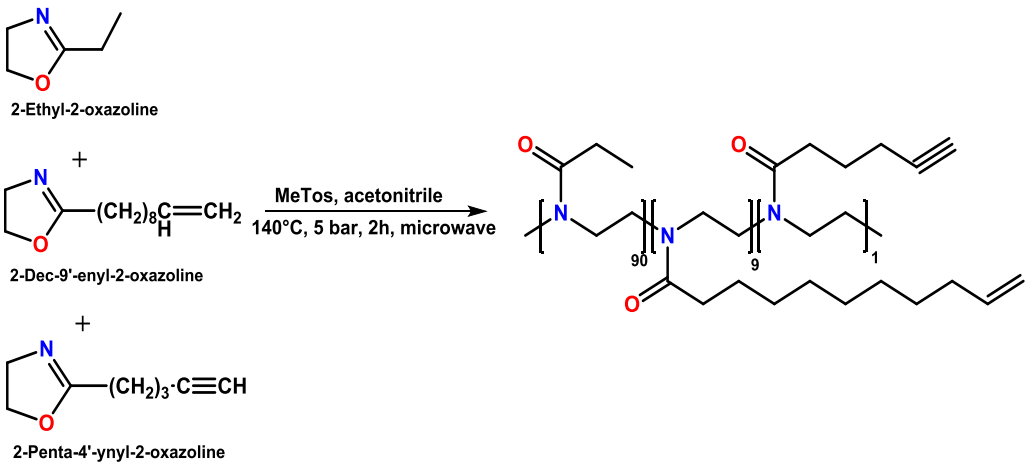

Scheme 16: Synthesis of pEtOx$_{90}$-*block*-p(DecOx$_9$-*stat*-PenOx$_1$).

A 5 mL Biotage reaction vial was dried in an oven at 80 °C for 30 minutes. Afterwards, the dried vessel was flushed with argon and 1.631 g (0.02 mol) EtOx, dissolved in 2 mL of acetonitrile, and 35.00 mg (1.8 mmol) MeOTs were weighed in under inert conditions. The vial was crimped and placed in the Biotage microwave reactor. After 5 s of pre-stirring, the

reaction mixture was heated to 140 °C for 1 h. Subsequently, 0.345 g (1.7 mmol) Dec$^{=}$Ox and 0.0255 g (0.2 mmol) Pen$^{\equiv}$Ox, mixed and dissolved in 1 mL acetonitrile, were added to the reaction vial under inert conditions. The mixture was pre-stirred for 5 s in the microwave reactor and then it was heated to 140 °C for 1 h. The solvent was evaporated under reduced pressure (< 2 mbar), and the polymer could be obtained as white solid.

^{1}H NMR (300 MHz, $CDCl_3$): δ = 5.79 (23H), 5.01-4.86 (46H), 3.44 (1020H), 2.34 (511H), 2.16 (4H), 2.01 (52H), 1.56 (52H), 1.27 (230H), 1.11 (687H).

^{13}C NMR (76 MHz, $CDCl_3$): δ = 174.6, 174.5, 174.0, 174.0, 114.2, 46.4, 45.9, 45.6, 45.4, 33.8, 28.8, 26.0, 9.5.

IR: (ATR) ν (cm^{-1}) = 2921, 2851, 2118, 1641, 1463, 1430, 1183, 1161, 909, 772, 721.

GPC: M_w = 5414 g·mol^{-1}; M_n =3880 g·mol^{-1}; PDI = 1.4.

8.5. Drug Deposition via the Huisgen Click-Reaction

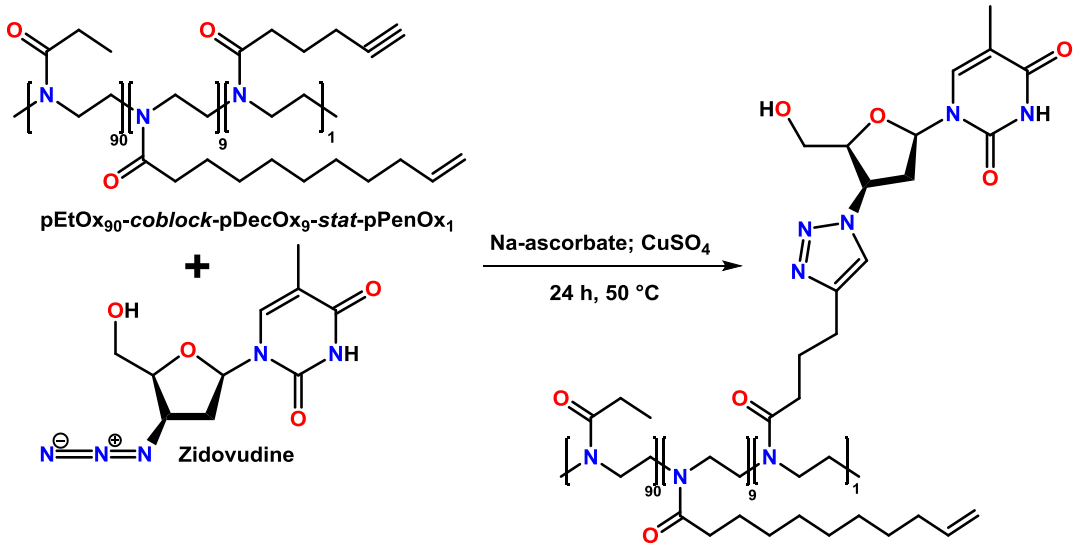

Scheme 17: Coupling of Zidovudine to pEtOx$_{90}$-*block*-p(DecOx$_9$-*stat*-PenOx$_1$) via the Huisgen Click-Reaction.

For the coupling of the polymer with Zidovudine, 5.9 mg (0.022 mmol, 0.95 equiv.) Zidovudine and 252.3 mg pEtOx$_{90}$-*block*-p(DecOx$_9$-*stat*-PenOx$_1$) (0.023 mmol, 1 equiv.) were dissolved in 10 ml DMF:water (5:1) in a 50 mL round bottom flask. After the addition of 44.5 mg (0.22 mmol) sodium-L-ascorbate and 27.3 mg (0.17 mmol) $CuSO_4$, the reaction mixture was stirred and heated to 50 °C. The color of the mixture changed from yellow to green after 1 h stirring, and finally it was turquois. After 24 h of stirring, the solvent was evaporated at reduced pressure and the solid residue was dissolved in DCM. The green solution was extracted with brine (3 times, 150 mL) and dried over Na_2SO_4. Afterwards, the solution was filtered. The solvent was evaporated under reduced pressure (< 2 mbar), and the solid product was dried under high vacuum for 1 d. Yield: 180.1 mg (0.016 mmol, 74%).

^{1}H-NMR (300 MHz, $CDCl_3$): δ = 8.08 (2H), 8.00 (2H), 5.77 (30H), 4.93 (60H), 3.44 (1324H), 2.95 (8H), 2.87 (7H), 2.34 (663H), 2.00 (67H), 1.58 (67H), 1.27 (298H), 1.11 (894H).

IR: (ATR) ν (cm^{-1}) = 3640**,** 2921, 2851, 2350, 2118, 1641, 1463, 1430, 1183, 1161, 1129, 772, 721.

8.6. Micelle Formation of Non-Crosslinked Amphiphiles

10 mg of each polymer were dissolved in 10 mL of acetone. Under vigorous stirring, 10 mL water were added drop wise to each solution. The clear solutions were dialyzed against water in a dialysis membrane (SpectraPor 4000-6000 Da) for 3 d.

8.7. Preparation of Crosslinked Micelles

8.7.1. pEtOx$_{95}$-*block*-pDec$^{=}$Ox$_5$

20 mg of the polymer were dissolved in 10 mL of acetone. 10 μL of photoinitiator and 0.77 μL of GDMA were added. Under vigorous stirring, 10 mL o fwater were added drop wise. The solution was dialyzed against water in a dialysis membrane (SpectraPor 4000-6000 Da) for 3 d, protected from light irradiation. Afterwards, the solution was transferred into a beaker and, under vigorous stirring, illuminated with UV light for 1 h.

8.7.2. pEtOx$_{90}$-*block*-pDec$^{=}$Ox$_{10}$

20 mg of the polymer were dissolved in 10 mL of acetone while the vial was protected from light irradiation. 10 μL of photoinitiator and 1.45 μL of GDMA were added. Under vigorous stirring, 10 mL of water were added drop wise. The solution was dialyzed against water in a dialysis membrane (SpectraPor 4000-6000 Da) for 3 d, protected from light irradiation. Afterwards, the solution was transferred into a beaker and, under vigorous stirring, it was illuminated with UV light for 1 h.

8.7.3. pEtOx$_{85}$-*block*-pDec$^{=}$Ox$_{15}$

20 mg of the polymer were dissolved in 10 mL of acetone, while the vial was protected from light irradiation. A drop of photoinitiator and 2.08 μL GDMA were added. Under vigorous stirring, 10 mL of water were added drop wise. The solution was dialyzed against water in a dialysis membrane

(SpectraPor 4000-6000 Da) for 3 d, protected from light irradiation. Afterwards, the solution was transferred into a beaker and, under vigorous stirring, it was illuminated with UV light for 1 h.

8.7.4. pEtOx$_{90}$-*block*-p(Dec$^{=}$Ox$_9$-*stat*-PenOx$_1$) + Zidovudine

10 mg of the polymer, which was coupled to Zidovudine, were dissolved in 10 mL of acetone. The vial was protected from light irradiation. A drop of photoinitiator and 0.7 µL of GDMA were added. Under vigorous stirring, 10 mL of water were added drop wise. The solution was dialyzed against water in a dialysis membrane (SpectraPor 4000-6000 Da) for 3 d, protected from light irradiation. Afterwards, the solution was transferred into a beaker and, under vigorous stirring, it was illuminated with UV light for 1 h.

9. References

[1] V.P. Torchilin: Structure and design of polymeric surfactant-based drug delivery systems. *Journal of Controlled Release*; **2001**, *73*, 137-172.

[2] M.C. Jones, J.C. Leroux: Polymeric micelles - a new generation of colloidal drug carriers. *European Journal of Pharmaceutics and Biopharmaceutics;* **1999**, *48*, 101-111.

[3] R.H. Müller: Colloidal Carriers for Contolled Drug Delivery and Targeting. *Wissenschaftliche Verlagsgesellschaft;* **1991**.

[4] K. Kataoka, A. Harada, Y. Nagasaki**,** *Adv. Drug Deliv. Rev*; **2001**, *47*, 1113-131.

[5] S. Schöttler, G. Becker, S. Winzen, T. Steinbach, K. Mohr, K. Landfester, V. Mailänder, F.R. Wurm: Protein adsorption is required for stealth effect of poly(ethylene glycol)- and poly(phosphoester)- coated nanocarriers. *Nature Nanotechnology;* **2016**, *11*, 372-377.

[6] R. Luxenhofer, Y. Han, A. Schulz, J. Tong, Z. He, A.V. Kabanova, R. Jordan: Poly(2-oxazoline)s as Polymer Therapeutics. *Macromol Rapid Commun;* **2012**, *15*, 1613-1631.

[7] B. Guillerm, V. Darcos, V. Lapinte, S. Monge, J. Coudane, J.J. Robin**:** Synthesis and evaluation of triazole-linked poly(e-cabrolactone)-graft-poly(2-methyl-2-oxazoline) copolymers as potential drug carriers. *Chem Comm;* **2012**.

[8] R. Luxenhofer, G. Sahay, A. Schulz, D. Alakhova, T.K. Bronich, R. Jordan, A.V. Kabanov: *J. Control Release*; **2011**, *153*, 73-82.

[9] D.A. Tomalia, G.R. Killat: *Encyclopedia of Polymer Science and Engineering.* s.l. : Wiley, **1985**, 680-739.

[10] B. Pidhatika, M. Rodenstein, Y. Chen, E. Rakhmatullina, A. Mühlebach, C. Acikgöz, M. Textor, R. Konradi**:** *Biointerphases.* **2010**, *7*, 1-15.

[11] E. Rossegger, V. Schenk, F. Wiesbrock: Design strategies for functionalized poly(2-oxazoline)s and derived materials. *Polymers (Basel);* **2013**, *5*, 956-1011.

[12] H.C. Kolb, M.G. Finn, K.B. Sharpless**:** Click Chemistry: Diverse Chemical Function from a Few Good Reactions. *Angew. Chemie - Int. Ed;* **2001**, *40*, 2004-2021.

[13] M. Fimberger, A. Behrendt, G. Jakopic, F. Stelzer, V. Kumbbaraci, F. Wiesbrock: Modification Pathways for Copoly(2-oxazoline)s Enabling Their Application as Antireflective Coatings in Photolithography. *Macromol. Rapid Commun;* **2016**, 37, 233-238.

[14] S. Gabriel: Zur Kenntnis des Bromäthylamins*. Berichte Der Dtsch. Chem. Gesellschaft*; **1889**, *22*, 1139-1154.

[15] H.-J. Krause, P. Neumann: Verfahren zur Herstellung von 2-Alkyl- bzw. 2-Alkenyloxazolinen*. EP 0 315 856 B1;* **1995**.

[16] H. Witte, W. Seeliger: Cyclische Imidsäureester aus Nitrilen und Aminoalkoholen*. Justus Liebigs Ann. Chem*; **1974**, *1974*, 996-1009.

[17] A. Gress, A. Völkel, H. Schlaad: Thio-Click Modification of Poly[2-(3-butenyl)-2-oxazoline]. *Macromolecules*; **2007**, *40*, 7928-7933.

[18] T.R. Dargaville, K. Lava, B. Verbraeken, R. Hoogenboom: Unexpected Switching of the Photogelation Chemistry in Cross-Linked Poly(2-oxazoline) Copolymers. *Macromolecules*; **2016**, *49*, 4774-4783.

[19] C. Petit, K.P. Luef, M. Edler, T. Griesser, J.M. Kremsner, A. Stadler, B. Grassl, S. Reynaud, F. Wiesbrock: Microwave-Assisted Syntheses in Recyclable Ionic Liquids: Photoresists Based on Renewable Resources. *ChemSusChem*; **2015**, *8*, 3401-3404.

[20] D.A. Tomalia, D. P. Sheetz: Homopolymerization of 2-alkyl- and 2-aryl-2-oxazolines. *J. Polym. Sci. Part A-1 Polym. Chem;* **1966***, 4*, 2253-2265.

[21] T. Kagiya, T. Maeda, K. Fukui, S. Narisawa: Ring Opening Polymerization of 2-substituted 2-Oxazolines. *Poly. Lett;* **1966**, *4*, 441-445.

[22] W. Seeliger, E. Aufderhaar, W. Diepers, R. Reinauer, R. Nehring, W. Thier, H. Hellmann**:** Recent Syntheses and Reactions of Cyclic Imidic Esters. *Angew. Chemie Int. Ed;* **1966**, *5,* 875-888.

[23] A. Levy, M. Litt: Polymerization of Cyclic Imino Ethers I. Oxazolines. *Polym. Lett;* **1967**, *5*, 871-879.

[24] F. Wiesbrock, R. Hoogenboom, C.H. Abeln, U.S. Schubert: Single-Mode Microwave Ovens as New Reaction Devices: Accelerating the Living Polymerization of 2-Ethyl-2-Oxazoline. *Macromol. Rapid Commun;* **2005***, 26*, 160-163.

[25] F. Wiesbrock, R. Hoogenboom, M. Leenen, S.F.G.M. Van Nispen, M. Van Der Loop, C.H. Abeln, A.M.J. Van Den Berg, U.S. Schubert: Microwave-Assisted Synthesis of a 4^2-Membered Library of Diblock Copoly (2-oxazolie)s and Chani-Extended Homo Poly(2-oxazoline)s and Their Thermal Characterization. *Macromolecules;* **2005***, 38,* 7957-7966.

[26] M. Glassner, D. R. D'Hooge, J. Young Park, P.H.M. Van Steenberge, B. D. Monnery, M.F. Reyniers, R. Hoogenboom: Systematic investigation of alkyl sulfonate initiators for the cationic ring-opening polymeriazation of 2-oxazolines revealing optimal combinations of monomers and initiators. *Eur. Polym. J;* **2015***, 65*, 298-304.

[27] M. Fimberger, K. Luef, C. Payerl, R. Fischer, F. Stelzer, M. Kállay, F. Wiesbrock: The pi-Electron Delocalization in 2-Oxazolines Revisited: Quantification and Comparison with Its Analogue in Esters. *Materials (Basel);* **2015***, 8*, 5383-5397.

[28] C. Ebner, T. Bodner, F. Stelzer, F. Wiesbrock: One decade of microwave-assisted polymerizations: Quo vadis? *Macromol. Rapid Commun; **2011**, 32*, 254-288.

[29] M. Litt, A. Levy, J. Herz: Polymerization of Cyclic Imino Ethers. X. Kinetics, Chain Transfer, and Repolymerization. *J. Macromol. Sci. Chem;* **1975**, *5*, 703-727.

[30] R. Hoogenboom, M.W.M. Fijten, H.M.L. Thijs, B.M. van Lankvelt, U.S. Schubert**:** Microwave-assisted synthesis and properties of a series of poly(2-alkyl-2-oxazoline)s. *Des. Monomers & Polym;* **2005***, 8*, 659-671.

[31] J.M. Kranenburg, C.A. Tweedie, R. Hoogenboom, F. Wiesbrock, H.M.L. Thijs, C.E. Hendriks, K. J. Van Viet, U.S. Schubert: Elastic moduli for a diblock copoly(2-oxazoline) library obtained by high-throughput screening. *J. Mater. Chem;* **2007**, *17*, 2713-2721.

[32] M.W.M. Fijten, J.M. Kranenburg, H.M.L. Thijs, R.M. Paulus, B.M. Van Lankvelt, J. De Hullu, M. Springintveld, D.J.G. Thielen, C.A. Tweedie, R. Hoogenboom, K.J. Van Vliet, U.S. Schubert, F.V. Jena, R. V March, V. Re, M. Recei, V. June: Synthesis and Structure - Property Relationships of Random and Block Copolymers: A Direct Comparison for Copoly(2-oxazoline)s; **2007**, 5879-5886.

[33] S. Wijnans, B.-J. de Gans, F. Wiesbrock, R. Hoogenboom, U.S. Schubert: Characterization of a Poly(2-oxazoline) Library by High-Throughput, Automated Contact-Angle Measurements and Surface-Energy Calculations. *Macromol. Rapid Commun;* **2004**, *25*, 1958-1962.

[34] S. Hoeppener, F. Wiesbrock, R. Hoogenboom, H.M.L. Thijs, U.S. Schubert**:** Morphologies of Spin-Coated Films of a Library of Diblock Copoly(2-oxazoline)s and Their Correlation to the Corresponding Surface Energies. *Macromol. Rapid Commun;* **2006***, 27*, 405-411.

[35] K. Kempe, E.F.-J. Rettler, R.M. Paulus, A. Kuse, R. Hoogenboom, U.S. Schubert**:** A systematic investigation of the effect of side chain branching on the glass transition temperature and mechanical properties of aliphatic (co-)poly(2-oxazoline)s. *Polymer (Guildf);* **2013**, *54*, 2036-2042.

[36] K. Kempe, S. Jacobs, H.M.L. Lambermont-Thijs, M.M.W.M. Fijten, R. Hoogenboom, U.S. Schubert: Rational Design of an Amorphous Poly(2-

oxazoline) with a Low Glass-Transition Temperature: Monomersynthesis, Copolymerization and Properties. *Macromolecules;* **2010**, *43*, 4098-4104.

[37] R. Hoogenboom, H.M.L. Thijs, M.W.M. Fijten, U.S. Schubert: Synthesis, characterization and cross-linking of a library of statistical copolymers based on 2-"soy alkyl"-2-oxazoline and 2-ethyl-2-oxazoline. *J. Polym. Sci. Part A Polym. Chem;* **2007**, *45*, 5371-5379.

[38] H.M.L. Lambermont-Thijs, M.W.M. Fijten, A.J. Van Der Linden, B.M. Van Lankvelt, M.M. Bloksma, U.S. Schubert, R. Hoogenboom: Efficient cationic ring-opening polymerization of diverse cyclic imino ethers: Unexpected copolymerization behavior. *Macromolecules;* **2011***, 44*, 4320-4325.

[39] R. Hoogenboom, F. Wiesbrock, M.a.M. Leenen, M. van der Loop, S.F.G.M. van Nispen, U.S. Schubert: Kinetic Investigations on Microwave-Assisted Statistical Terpolymerizations of 2-Oxazoline Monomers. *Aust. J. Chem;* **2007***, 60*, 656.

[40] R. Hoogenboom, H.M.L. Thijs, M.W.M. Fijten, B.M.V.A.N. Lankvelt, U.S. Schubert: One-Pot Synthesis of 2-Phenyl-2-oxazoline-Containing Quasi-Diblock Copoly(2-oxazoline)s under Microwave Irradiation. **2006**, 416-422.

[41] C.E. Hoyle, C.N. Bowman**:** Thiol-En-Klickchemie. *Angew. Chemie;* **2010***, 122*, 1584-1617.

[42] M. Fimberger, V. Schenk, E. Rossegger, F. Wiesbrock: UV-Induced Crosslinking of Poly[2-(2'-Norbornenyl)-2-oxazoline]s. *Period. Polytech. Chem. Eng;* **2014***, 58*, 69.

[43] A. Gress, A. Völkel, H. Schlaad**:** Thio-Click Modification of Poly[2-(3'-butenyl)-2-oxazoline]. *Macromolecules;* **2007***, 40*, 7928-7933.

[44] K. Kempe, A. Vollrath, H.W. Schaefer, T.G. Poehlmann, C. Biskup, R. Hoogenboom, S. Hornig, U.S. Schubert: Multifunctional poly(2-oxazoline) nanoparticles for biological applications. *Macromol. Rapid Commun;* **2012***, 31*, 1869-1873.

[45] J. Rueda, R. Suica, H. Komber, B. Voit: Synthesis of new poly(methyl-2-oxazoline) hydrogels by the "macroinitiator" method. *Macromol. Chem. Phys;* **2003**, 204, 954-960.

[46] K.P. Luef, C. Petit, B. Ottersböck, G. Oreski, F. Ehrenfeld, B. Grassl, S. Reynaud, F. Wiesbrock. UV-mediated thiol-ene click reactions for the synthesis of drug-loadable and degradable gels based on copoly(2-oxazoline)s. *Eur. Polym. J;* **2017***, 88*, 701-712.

[47] T.R. Dargaville, R. Forster, B.L. Farraguia, K. Kempe, L. Voorhaar, U.S. Schubert, R. Hoogenboom: Poly(2-oxazoline) hydrogel monoliths via thiol-ene coupling. *Macromol. Rapid. Commun;* **2012***, 33*, 1695-1700.

[48] A.M. Kelly, A. Hecke, B. Wirnsberger, F. Wiesbrock: Synthesis of Poly(2-oxazoline)-Based Hydrogels with Tailor-Made Swelling Degrees Capable of Stimuli-Triggered Compound Release. *Macromol. Rapid Commun;* **2011***, 32*, 1815-1819.

[49] T.R. Dargaville, B.G. Hollier, A. Shokoohmand, R. Hoogenboom**:** Poly(2-oxazoline) hydrogels as next generation three-dimensional cell supports. *Cell. Adhes. Migr*; **2014**, *8*, 88-93.

[50] J.M. Havard, M. Yoshida, D. Pasini, N. Vladimirov, J.M.J. Frechet, S. Yamada, K. Patterson, D.R. Medeiros, C.G. Willson, J.D. Byers: Design of Photoresists with Reduced Environmental Impact. 1. Water-Soluble Resists Based on Photo-Cross-Linking of Poly(2-Isopropenyl2-oxazoline). *J. Polym. Sci. Part A Polym. Chem;* **1999**, *37*,1225-1236.

[51] V. Schenk, L. Ellmaier, E. Rossegger, M. Edler, T. Griesser, G. Weidinger, F. Wiesbrock: Water-Developed Poly(2-oxazoline)-Based Negative Photoresists. *Macromol. Rapid Commun;* **2012**, *33*, 396-400.

[52] M. Fimberger, I.A. Tsekmes, R. Kochetov, J.J. Smit, F. Wiesbrock: Crosslinked poly(2-oxazoline)s as "green" materials for electronic applications. *Polymers (Basel);* **2016**, *8*, 1-12.

[53] E. Saxon, C.R. Bertozzi: Cell Surface Engineering by a modified Staudinger Reaction. *Science;* 2000, 287, 2007-2010.

[54] V.V. Rostovtsev, L.G. Green, V.V. Fokin, K.B. Sharpless: A Stepwise Huisgen Cycloaddition Process: Copper(I)-Catalyzed Regioselective “Ligation” of Azides and Terminal Alkynes. *Angew. Chem. Int. Ed;* **2002**, *41*, 2596-2599.

[55] M.Peer: *Spec. Chem. Mag.* **1998**, *18*, 256-263.

[56] V. D. Bock, H. Hiemstra, J.H. van Maarseveen**:** Cu1-Catalyzed Alkyne-Azide "Click" Cycloadditions from a Mechanistic and Synthetic Perspective. *Eur. J. Org. Chem;* **2006**, 51-68.

[57] K.V. Gothelf, K. A. Jorgensen**:** *Chem. Rev;* **1998**, 98, 863-909.

[58] A.R. Katritzky, S.K. Singh**:** *J. Org. Chem;* **2002**, 9077-9079.

[59] J. Bastide, O. Henri-Rousseau: *Bull. Soc. Chim. Fr;* **1973**, 2294-2296.

[60] P. Appukkuttan, W. Dehaen, V.V. Fokin, E. van der Eycken: A Microwave-Assisted Click Chemistry Synthesis of 1,4-Disubstituted 1,2,3-Triazoles via a Copper(I)-Catalyzed Three-Component Reaction. *Org. Lett*; **2004**, *6*, 4223-4225.

[61] C.W. Tornae, C. Christensen, M. Meldal**:** Peptidotriazoles on Solid Phase: [1,2,3]-Triazoles by Regiospecific Copper(I)-Catalyzed 1,3-Dipolar Cycloadditions of Terminal Alkynes to Azides. *J. Org. Chem;* **2002**, *67*, 3057-3064.

[62] F. Himo, T. Lovell, R. Hilgraf, V.V. Rostovtsev, L. Noodleman, K.B. Sharpless, V.V. Fokin: Copper(I)-Catalyzed Synthesis of Azoles. DFT Study Predicts Unprecedented Reactivity and Intermediates. *J. Am. Chem. Soc;* **2005***, 127*, 210-216.

[63] R. Luxenhofer, R. Jordan: Click Chemistry with Poly(2-oxazoline)s. *Macromolecules.* **2006**, *39*, 3509-3516.

[64] K. Kempe, C. Weber, K. Babiuch, M. Gottschaldt, R. Hoogenboom, U. S. Schubert: Responsive glycol-poly(2-oxazoline)s: Synthesis, cloud point tuning and lecitin binding. *Biomacromolecules;* **2011**, *12*, 2591-2600.

[65] F. Manzenrieder, R. Luxenhofer, M. Retzlaff, R. Jordan, M.G. Finn**:** Stabilization of virus like particles with poly(2-oxazoline)s. *Angew. Chem. Int. Ed;* **2011**, *50*, 2601-2605.

[66] M.W.M. Fijten, C. Haensch, B.M. van Lankvelt, R. Hoogenboom, U.S. Schubert: Clickable poly(2-oxazoline)s as versatile building blocks. *Macromol. Chem. Phys*; **2008**, *209*, 1887.

[67] M. A. Cortez, S. M. Grayson: *Polym. Mater. Sci. Eng**;*** **2008**, *98,* 436.

[68] G. Volet, T.X. Lav, J. Babinot, C. Amiel**:** Click-Chemistry: An Alternative Way to Functionalize Poly(2-methyl-2-oxazoline). *Macromol. Chem. Phys;* **2011**, *212*, 118-124.

[69] B. Guillerm, V. Darcos, V. Lapinte, S. Monge, J. Coudane, J.J. Robin: Synthesis and evaluation of triazole-linked poly(e-caprolactone)-graft-poly(2-methyl-2-oxazoline) copolymers as potential drug carriers. *Chem. Commun;* **2012**, *48*, 2879-2881.

[70] K.L. Mittal, B. Lindmann: Surfactants in Solution. *Plenum Press;* 1991*, 1-3*.

[71] M.C. Jones, J.C. Leroux: Polymeric Micelles- a new generation of colloidal drug carriers. *Eur. J. Pharm. Biopharm;* **1999***, 48*, 101-111.

[72] P. Wang, S. Pei, M. Wang, Y. Yan, X. Sun, J. Zhang**:** Coarse-grained molecular dynamics study on the self-assembly of Gemini surfactants: the effect of spacer length. *Phys.Chem.Chem.Phys;* **2017***, 19*, 4462-4468.

[73] J.N. Israelachvil, D.J. Mitchell, B.W. Ninham: Theory of Self-Assembly of Hydrocarbon Amphiphiles into Micelles and Bilayers. *J. Chem. Soc. , Faraday Trans 2*; **1976**, *72*, 1525-1568

[74] P.H. Elworthy, A.T. Florence, C.B. Macfarlane**:** Solubilization by Surface Active Agents; **1968**

[75] L. Zhang, A. Eisenberg: Multiple morphologies of "crew-cut" aggregates of polystyrene-b-poly(acrylic acid) block copolymers. *Science;* **1995***, 268*, 1728-1731.

[76] S. Cai, K. Vijayan, D. Cheng, E.M. Lima, D.E. Discher**:** Micelles of Different Morphologies - Advantages of Worm-like Filomicelles of PEO-PCL in Paclitaxel Delivery. *Pharmaceutical Research;* **2007**, *24*, 2099-2109

[77] C.M. Marques: Bunchy Micelles. *Langmuir;* **1997**, *13*, 1430-1433.

[78] C. Allen, D. Maysinger, A. Eisenberg: Nano-engineering block copolymer aggregates for drug delivery. *Coll. Surf. B: Biointerf;* **1999**, *16*, 1-35.

[79] C. Allen, Y. Yu, D. Maysinger, A. Eisenberg: Polycaprolactone-b-poly(ethylene oxide) block copolymer micelles as a novel drug delivery vehicle for neurotrophic agents. *Bioconj. Chem;* **1998**, *9*, 564-572.

[80] K. Yu, L. Zhang, A. Eisenberg: Novel morphologies of 'crew-cut' aggregates of amphiphilic diblock copolymers in dilute solutions. *Langmuir;* **1996**, *12*, 5980-5984.

[81] N.S. Cameron, M.K. Corbierre, A. Eisenberg: Asymmetric amphiphilic block copolymers in solution: a morphological wonderground. *Can. J. Chem;* **1999**, *77*, 1311-1326.

[82] L. Zhang, K. Yu, A. Eisenberg: Ion-induced morphological changes in 'crew-cut' aggregates of amphiphilic block copolymers. *Science;* **1996**, *272*, 1777-1779.

[83] L. Zhang, C. Bartles, K. Yu, H. Shen, A. Eisenberg**:** Mesosized crystal-like structure of hexagonally packed hollow hoops by solution self-assembly of diblock copolymers. *Phys. Rev. Lett;* **1997***, 79*, 5034-5037.

[84] Z. Gao, A. Eisenberg**:** A model of mizellation for block copolymers in solutions. *Macromolecules;* **1993**, *26*, 7353-7360.

[85] M. Yokoyama: Block copolymers as drug carriers. *CRC Crit. Rev. Ther. Drug Carrier Syst;* **1992**, *9*, 213-248.

[86] J. Sinnko: *Martin's "Physical Pharmacy and Pharmaceutical Sciences"* Baltimore : Lippincott Williams & Wilkins, **2006**, *9.*

[87] D.G. Hall: *Nonionic Surfactants Physical Chemistry.* New York : Marcel Dekker, **1967**, *13*.

[88] L. Chen, S.Y. Lin, C. Huang; *Colloids Surf A Physiochem Eng Asp*; **1998**, *135*, 175-181.

[89] E. Mohajeri, G.D. Noudeh**.**: Effect of Temperature on the Critical Micelle Concentration and Mizellization Thermodynamic of Nonionic Surfactants: Polyoxyethylene Sorbitan Fatty Acid Esters. *E-Journal of Chemistry;* **2012**, ,*9(4)*, 2268-2274.

[90] N.J. Turro, C.J. Chung: Photoluminescents probes for water soluble polymers. Pressure and temperature effect on a polyol surfactant. *Macromolecules;* **1984**, *17*, 2123-2126.

[91] I. Astafieva, X. Zhong, A. Eisenberg**:** Critical micellization phenomena in block polyelectrolyte solution. *Macromolecules;* **1993**, *26*, 7339-7352.

[92] R. Takahashi, T. Sato, K. Terao, X.-P. Qiu, F.M. Winnik**:** Self-association of a thermosensitive poly(alkyl-2-oxazoline) block copolymer in queous solution. *Macromolecules;* **2012**, *45*, 6111-6119.

[93] O. Casse, A. Shikilnyy, J. Linders, C. Mayer, D. Häussinger, A. Völkel, A.F. Thünemann, R. Dimova, H. Cölfen, W. Meier: Solution behavior of double-hydrophilic block copolymers in dilute aqueous solution. *Macromolecules.* 2012, Vol. 45, pp. 4772-4777.

[94] L.T.T. Trinh, H.M.L. Lambermont-Thijs, U.S. Schubert, R. Hoogenboom, A.L. Kjoniksen: Thermorespnsive poly(2-oxazoline) block copolymers exhibiting two cloud points: Complex multistep assembly behavior. *Macromolecules;* **2012**, *45*, 4337-4345.

[95] C.A. Fustin, N. Lefèvre, R. Hoogenboom, U.S. Schubert, J.-F. Gohy: Surface micellization of poly(2-oxazoline)s based copolymers containing a crystallizable block. *J. Colloid Interface Sci;* **2009**, *332*, 91-95.

[96] R. Ivanova, T. Komenda, T.B. Bonné, K. Lüdtke, K. Mortensen, P.K. Pranzas, R. Jordan, C.M. Papadakis: Micellar structures of hydrophilic/lipophilic and hydrophilic7fluorophilic poly(2-oxazoline) diblock copolymers in water. *Macromol. Chem. Phys;* **2008**, *209*, 2248-2258.

[97] O. Nuyken, P. Persigehl, R. Weberskirch**:** Amphiphilic poly(oxazoline)s-synthesis and application for micellar catalysis. *Macromol. Symp;* **2002**, *177*, 163-173.

[98] H. Huang, R. Hoogenboom, M.A.M. Leenen, P. Guillet, A.M. Jonas, U.S. Schubert, J.-F. Gohy**:** Solvent-induced morphological transition in core-cross-linked block copolymer micelles. *J. Am. Chem. Soc;* **2006**, *128*, 3784-3788.

[99] R. Hoogenboom, F. Wiesbrock, H. Huang, M. a. M. Leenen, H.M.L. Thijs, S.F.G.M. van Nispen, M. van der Loop, C.-A. Fustin, A.M. Jonas, J. -F. Gohy, U.S. Schubert: Microwave-Assisted Cationic Ring-Opening Polymerization of 2-Oxazolines: A Powerful Method for the Synthesis of Amphiphilic Triblock Copolymers. *Macromolecules;* **2006***, 39*, 4719-4725.

[100] R. Hoogenboom, F. Wiesbrock, M.A.M. Leenen, H.M.L. Thijs, H. Huang, C.-A. Fustin, P. Guillet, J.-F. Gohy, U.S. Schubert: Synthesis and Aqueous Micellization of Amphiphilic Tetrablock Ter- and Quarterpoly(2-oxazoline)s. *Macromolecules;* **2007***, 40*, 2837-2843.

[101] T.B. Bonné, K. Lüdtke, R. Jordan, C.M. Papadakis: Effect of polymer architecture of amphiphilic poly(2-oxazoline) copolymers on the aggregation and aggregate structure. *Macromol. Chem. Phys;* **2007**, *208*, 1402-1408.

[102] C. Cuerro-Sanchez, J.-F. Gohy, C. D'Haese, H. Thijs, R. Hoogenboom, U.S. Schubert: Controlled thermoreversible transfer of poly(oxazoline) micelles between an ionic liquid and water. *Chem. Commun;* **2008**, 2753-2755.

[103] K. Kempe, A. Baumgäertel, R. Hoogenboom, U.S. Schubert: Design of new amphiphilic triblock copoly(2-oxazoline)s containing a fluorinated segment. *J. Polym. Sci. A Polym. Chem;* **2010**, *48*, 5100-5108.

[104] R. Luxehofer, A. Schulze, C. Roques, S. Li, T.K. Bronich, E.V. Batrakova, R. Jordan, A.V. Kabanov: Doubly amphiphilic poly(2-oxazoline)s as high-capacity delivery system for hydrophobic drugs. *Biomaterials;* **2010**, *31*, 4972-4979.

[105] H.-J. Choi, E. Brooks, C.D. Montemagno**:** Syntehsis and characterization of nanoscale biomimetic polymer vesicles and polymer membranes for bioelectronics applications. *Nanotechnology;* **2005**, *16*, 143-149.

[106] C.V. De Macedo, M.S. da Silva, T. Casimiro, E.J. Cabrita, A. Aguiar-Ricardo: Boron trifluoride catalyzed polymerisation of 2-substituted-2-oxazolines in supercritical carbon dioxide. *Green Chem;* **2007**, 9, 948-953.

[107] D. Schönfelder, K. Fischer, M. Schmidt, O. Nuyken, R. Weberskirch: Poly(2-oxazoline)s functionalized with palladium carbene complexes: Soluble, amphiphilic polymer supports for C-C coupling reactions in water. *Macromolecules;* **2005**, *38,* 254-262.

[108] Y. Han, Z. He, A. Schulz, T.K. Bronich, R. Jordan, R. Luxenhofer, A.V. Kabanov**:** Synergistic combinations of multiple chemotherapeutic agents in high capacity poly(2-oxazoline) micelles. *Mol. Pharm;* **2012**, *9*, 2302-2313.

[109] D.K. Owens, R.C: Wendt: Estimation of the surface free energy of polymers. *J. Appl. Polym. Sci;* **1969**, *13*, 1741-1747.

[110] L. Hsiao, H.N. Dunning, P.B. Lorenz: Critical Micelle Concentration Of Polyethylatet Non-Ionic Detergents. *J. Phys. Chem;* **1956**, *60* (5), 657-660.

[111] W.J. Moore, D.O. Hummel: *Physical Chemistry,* Walter deGruyter **1986***, 4*

[112] H.G. Elias: *Makromoleküle - Physikalische Strukturen und Eigenschaften.* USA : WILEY-VCH, **2001**, *2.*

10. Appendix

10.1. List of Abbreviations

$CHCl_3$	chloroform
CL	crosslinker
CMC	critical micelle concentration
CMT	critical micelle temperature
CROP	cationic ring-opening polymerization
Dec$^{=}$Ox	2-dec-9´-enyl-2-oxazoline
DCM	dichloromethane
DMF	dimethylformamide
DLS	dynamic light scattering
Et_3N	triethylamine
EtOH	ethanol
EtOx	2-ethyl-2-oxazoline
GDMA	glycol dimercaptoacetate
MeOH	methanol
MeOTs	methyl tosylate
MW	microwave
NonOx	2-nonyl-2-oxazoline
pDec$^{=}$Ox	poly(2-dec-9'-enyl-2-oxazoline)
pEtOx	poly(2-ethyl-2-oxazoline)
pPen$^{\equiv}$Ox	poly(2-pent-4-ynyl-2-oxazoline)
pOx	poly(2-oxazoline)
PI	photoinitiator
SANS	small angle neutron scattering
SAXS	small angle x-ray scattering
T_g	Glass-transition temperature
THF	tetrahydrofurane
UV light	ultraviolet light

10.2. List of Tables

10.3. List of Figures

10.4 List of Schemes